

The case for old basaltic shergottites

Audrey Bouvier^{a,*}, Janne Blichert-Toft^b, Jeffrey D. Vervoort^c,
Philippe Gillet^b, Francis Albarède^b

^a *University of Arizona, Department of Geosciences, Tucson, AZ 85721, USA*

^b *Ecole Normale Supérieure, Laboratoire des Sciences de la Terre, 69007 Lyon, France*

^c *Washington State University, School of Earth and Environmental Sciences, Pullman, WA 99164, USA*

Received 10 June 2007; received in revised form 22 October 2007; accepted 4 November 2007

Available online 17 November 2007

Editor: G.D. Price

Abstract

The crystallization age of shergottites is currently not agreed upon. Although mineral ^{87}Rb – ^{87}Sr , ^{147}Sm – ^{143}Nd , ^{176}Lu – ^{176}Hf , and U–Pb isochrons all give very young ages, typically in the range of 160–180 Ma, ^{207}Pb – ^{206}Pb data support a much older crystallization age at 4.1 Ga, which is consistent with published whole-rock ^{87}Rb – ^{87}Sr data on basaltic shergottites. Different isotopic systems present different complexities, but crater-counting chronology, which shows that a substantial fraction of the Martian surface was resurfaced during the late heavy bombardment, is in favor of an old Martian lithosphere with ages in accordance with Pb–Pb and Rb–Sr isotopic data. A ~ 4.1 Ga Pb–Pb age of shergottites also agrees with the ^{142}Nd and ^{182}W anomalies found in these rocks and concur with the presence of an actively convecting mantle during the first 500 Myr of the planet's history.

We here present new Sm–Nd, Lu–Hf, and Pb–Pb mineral isochrons for the basaltic shergottites Shergotty and Los Angeles complementing our previous results on Zagami [Bouvier A., Blichert-Toft J., Vervoort J.D. and Albarède F. (2005). The age of SNC meteorites and the antiquity of the Martian surface, *Earth Planet. Sci. Lett.* 240, 221–233]. The internal ^{147}Sm – ^{143}Nd and ^{176}Lu – ^{176}Hf isochrons give young ages of, respectively, 172 ± 40 (MSWD=2.0) and 188 ± 91 (MSWD=3.1) for Shergotty, and 181 ± 13 (MSWD=0.14) and 159 ± 42 (MSWD=0.01) for Los Angeles. In contrast, the Pb isotope compositions of the leached whole-rock fragments and maskelynite separates of Shergotty and Los Angeles fall on the whole-rock isochron previously established for Zagami and other shergottite samples and collectively yield a Pb–Pb age of 4050 ± 70 Ma for the crystallization of the basaltic shergottite suite. The contrast between the ~ 170 Ma ages of internal isochrons and the 4.1 Ga age supported by Pb–Pb and ^{87}Rb – ^{87}Sr on whole-rocks simply reflects that the younger age dates the perturbation of a suite of rocks of Noachian age. The internal Rb–Sr, Sm–Nd, Lu–Hf, and U–Pb errorochrons are heavily biased by the presence of disseminated phosphate minerals and inclusions, for which D/H ratios ($\delta\text{D} \sim +4600\%$) indicate strong interaction with Martian subsurface waters. In contrast, baddeleyite, occasionally present in SNCs and also having extremely young U–Pb ages, reflect resetting under the shock conditions that prevailed either during shergottite extraction from the planet or from impacts associated with a major break-up

* Corresponding author. Tel.: +1 480 965 7762; fax: +1 480 965 8102.

E-mail address: audrey.bouvier@asu.edu (A. Bouvier).

¹ Present address: School of Earth and Space Exploration, Arizona State University, Tempe, AZ 85287, USA.

event of planetesimals in the main asteroid belt. We finally also re-examine ^{39}Ar – ^{40}Ar data on SNC meteorites and suggest that they as well support old crystallization ages.

© 2007 Elsevier B.V. All rights reserved.

Keywords: Mars; shergottite; chronology; impact; aqueous alteration; Pb isotopes; Hf isotopes; Nd isotopes

1. Introduction

The SNC meteorites (historically Shergotty–Nakhla–Chassigny) are widely considered to have been derived from Mars. Oxygen isotopes indicate that these rocks are from a single planetary body (Clayton and Mayeda, 1983; Franchi et al., 1999), and the abundance patterns of gases (particularly rare gases) occluded in pockets of shock melt (Bogard and Johnson, 1983; Pepin, 1985) are very similar to the Martian atmosphere as analyzed by the Viking landers (Owen, 1976). Furthermore, the apparently young (<1 Ga) radiometric ages of these meteorites call for a parent planet with equally young volcanic activity, which at first glance seems to fit the well-preserved morphology of Martian volcanoes. A broad consensus has emerged over the last two decades that nakhlites and chassignites are ~1.3 Ga old, whereas shergottites are much younger, on the order of a few hundred million years. Two distinctly different classes of shergottites have been identified, basaltic and lherzolitic. Only the former will be discussed in detail here. Numerous isotopic data from different long-lived radiogenic systems (^{87}Rb – ^{87}Sr , ^{147}Sm – ^{143}Nd , ^{176}Lu – ^{176}Hf , U–Pb), as well as exposure ages, have been obtained for basaltic shergottites and are summarized by Nyquist et al. (2001). Most mineral (internal) isochron ages cluster around 180 Ma and 330–475 Ma (Nyquist et al., 2001), which, since Jones (1986), generally is taken as the crystallization ages of these rocks. The whole-rock data, however, are inconsistent with this interpretation: scatter makes the ^{147}Sm – ^{143}Nd data essentially useless for dating purposes, while the >4 Ga age indicated by the shergottite ^{87}Rb – ^{87}Sr whole-rock errorchron so far has been seen as reflecting the time of reservoir differentiation (Borg et al., 1997, 2005; Shih et al., 1982). Exposure ages are fully consistent from one chronometer to another (Nyquist et al., 2001), thus bestowing strong credibility on this body of data. Importantly, they define multiple groups, which exclude the interpretation that the shergottites could have been extracted from the Martian surface or subsurface by a single impact event.

Because volcanic rocks and sediments are absent from the samples suspected to originate from Mars, it

seems likely that shergottites, the most abundant type among the SNC meteorites and equivalent to plutonic rocks, represent a dominant lithology of the planetary subsurface. Blichert-Toft et al. (1999) and more recently Bouvier et al. (2005) have questioned the evidence that basaltic shergottites crystallized as shallow intrusions as recently as 180 Myr ago. Our previous arguments can be combined with additional evidence and summarized as follows:

Regardless of the uncertainties, cratering chronology (Barlow, 1988; Hartmann and Neukum, 2001; Werner et al., 2005) and stratigraphy (Tanaka and Scott, 1987; Tanaka et al., 1992) assign an age greater than 2 Ga to most of the Martian surface. As discussed by Nyquist et al. (1998, 2001), the inordinate number of apparently young shergottites contrasts with the relatively small proportion of adequately young terrains. Hartmann and Neukum (2001) reiterate that “only a modest percentage of the known volcanics are younger than 1.3 Gyr [i.e., the age of nakhlites]”. The diversity of exposure ages (Nyquist et al., 2001) thus leaves unanswered the question of how multiple impacts could have extracted nearly exclusively young material from the Martian surface.

Evidence of old Pb–Pb ages in basaltic shergottites, for which the labile component (dominated by apatite) has been removed by acid leaching, is overwhelming: leached maskelynite (the current amorphous state of plagioclase left by impact) and other minerals give ages in excess of 4 Ga. A tentative case for an old component was first made by Chen and Wasserburg (1986a), and later by Jagoutz (1991) for basaltic shergottites, and then again by Misawa et al. (1997) for the lherzolitic shergottite Y-793605. Recently, Bouvier et al. (2005) produced a statistically significant Pb–Pb isochron for Zagami with an age of 4.048 ± 0.017 Ga and observed that Pb from Los Angeles, EETA 79001, and Shergotty also fell on –or very near– the Zagami isochron. Likewise, excellent linear arrays were obtained in Pb–Pb isochron plots by Gaffney et al. (2007) for the most depleted member of the basaltic shergottite suite, QUE 94201, with correlation coefficients >0.999, but their 4.3 Ga age were dismissed as valid isochrons by the authors who rather consider these alignments as contamination artifacts.

The preservation of extinct radioactivity anomalies in shergottites, notably ^{142}Nd and ^{182}W (Foley et al., 2005; Harper et al., 1995; Kleine et al., 2004; Lee and Halliday, 1997), is perplexing if these meteorites are young. For such anomalies to have been preserved until the recent past in the mantle source of young shergottite magmas, mantle convection must have been either extremely sluggish or virtually non-existent for the entire 4.5 Gyr of the planet's history. In the light of evidence of an active dynamo during the first 500 Myr of Martian history (Connerney et al., 2001; Weiss et al., 2002), such a scenario seems unlikely.

Unleached whole-rock ^{87}Rb – ^{87}Sr data for shergottites define an errorchron with an apparent age in excess of 4 Ga (Borg et al., 1997, 2005; Shih et al., 1982).

Other indications of old ages include 4.0 to 2.5 Ga fission tracks in phosphate grains (Rajan et al., 1986) and K–Ar and ^{39}Ar – ^{40}Ar ages in excess of emplacement ages (Bogard and Garrison, 1999; Mathew et al., 2003; Walton et al., 2007).

The debate about the true age of shergottites was fueled again recently by the reporting of young Pb–Pb ages on baddeleyite in basaltic shergottites (Herd et al., 2007; Misawa and Yamaguchi, 2007). In order to evaluate this new line of evidence, we undertook a combined Pb–Pb, Sm–Nd, and Lu–Hf isotope study of two fragments of Los Angeles and Shergotty to complement our earlier results for Zagami. Our new data confirm that, although the Sm–Nd and Lu–Hf ages are young, hence in accordance with previous results, the Pb isotope compositions are all consistent with the ~ 4.1 Ga isochron defined previously by Zagami (Bouvier et al., 2005). In the following discussion we review ages from the shergottite literature and argue that they allow us to maintain the claim (Bouvier et al., 2005) that basaltic shergottites are ancient rocks in full agreement with the old ages estimated by crater size-frequency for most of the Martian surface.

2. Analytical techniques

We analyzed the Pb–Pb, Sm–Nd, and Lu–Hf isotope compositions of whole-rocks and mineral separates (maskelynite, augite, and pigeonite) from a 2.8 g piece of the basaltic shergottite Shergotty (fall) obtained from the Museum National d'Histoire Naturelle (MNHN, sample #430) and a 2.3 g piece of the basaltic shergottite Los Angeles (find) obtained from the American Museum of National History (AMNH). The analytical techniques employed for this work, carried out at the Ecole Normale Supérieure in Lyon and the Lunar and Planetary Laboratory in Tucson, were identical to those

reported in Bouvier et al. (2005) with the exception that a Nu Plasma HR MC-ICP-MS coupled with a desolvating nebulizer DSN-100 was used for isotopic analysis in place of the now retired Plasma 54. Blank levels posed a limitation to our pyroxene Pb isotope data for the following reason: because of limited availability of sample material, it was necessary to separate Pb, Sm, Nd, Lu, and Hf from the same sample dissolutions. While this in itself is not a problem, in order to achieve complete sample dissolution and sample-spike equilibration for the Sm–Nd and Lu–Hf parts of the combined analytical work, we were constrained to using steel-jacketed Teflon bombs for sample digestion and this step results in higher Pb blanks than if the samples could have simply been dissolved in PFA beakers (see discussion about blank levels of high-pressure bombs in Bouvier et al. (2007)). On closer inspection of literature Pb isotope data, however, augite and pigeonite separates are commonly inconsistent with other mineral phases (e.g., oxides and pyroxene residues of Zagami in Fig. 4 of Borg et al. (2005) and pyroxene residues of Shergotty in Fig. 1 of Chen and Wasserburg (1986a)). In contrast, blank participation was comparatively low for the maskelynite and whole-rock Pb isotope data (sample/blank ratios of ~ 300 – 700 for maskelynite and whole-rock residues, while of the order of ~ 10 – 100 for pyroxene residues; see Table 1 for blank corrections on Pb isotope compositions when applied), and negligible for leachate Pb isotope data, as well as for the Sm–Nd and Lu–Hf isotope data (total procedural blanks were better than 20 pg for Sm, Nd, Lu, and Hf, and amounted to 5 pg for Pb when sample dissolution had been done in PFA beakers instead of in bombs, which was the case for all the leachates and whole-rock fragment 3 of Los Angeles). A full description of the analytical procedures (leaching, dissolution, separation, and mass spectrometry) is given in Bouvier et al. (2005).

The ages presented here were all calculated with the Isoplot software (Ludwig, 2001) using external reproducibilities (Tables 1 and 2) as errors except when internal errors were larger.

3. Results

The Sm–Nd and Lu–Hf isotope data are presented in Table 2. Internal isochrons combining results on unleached whole-rock powder and leached maskelynite, pigeonite, and/or augite separates from Shergotty give a Sm–Nd age of 172 ± 40 (MSWD=2.0) (Fig. 1a) and a Lu–Hf age of 188 ± 91 (MSWD=3.1) (Fig. 1b). The precision on the Lu–Hf age can be improved to 188 ± 24 Ma (MSWD=0.01) if the whole-rock (WR2b in

Table 1
Pb isotope data for Shergotty and Los Angeles

Sample	Fraction ^a	Weight ^b (g)	Pb ^c (ppm)	²⁰⁶ Pb/ ²⁰⁴ Pb ^d Uncorr.	²⁰⁶ Pb/ ²⁰⁴ Pb ^{d,e} Corr.	2σ% SE	²⁰⁷ Pb/ ²⁰⁴ Pb ^{d,e} Corr.	2σ% SE	²⁰⁸ Pb/ ²⁰⁴ Pb ^{d,e} Corr.	2σ% SE	²⁰⁷ Pb/ ²⁰⁶ Pb ^{d,e} Corr.	2σ% SE	
Shergotty	Whole-rock 2a R	0.123	0.16	14.6661	14.6511	0.0005	13.6809	0.0005	34.7805	0.0013	0.933785	0.0008	
	Wash fragment 2 L0	–	–	–	18.3168	0.0006	15.6341	0.0007	38.4120	0.0022	0.853541	0.0013	
	L1	0.03	0.62	–	17.8370	0.0003	15.3554	0.0004	37.9675	0.0012	0.860886	0.0008	
	L2	0.03	1.1	–	17.7330	0.0009	15.2705	0.0008	37.8565	0.0022	0.861131	0.0008	
	Whole-rock 2b	0.140	1.7	17.3647	17.3626	0.0005	15.0980	0.0006	37.4875	0.0015	0.869568	0.0010	
	Pigeonite R	0.302	0.10	15.5822	15.5398	0.0006	14.1678	0.0006	35.6408	0.0019	0.911708	0.0011	
	L1	0.08	2.5	–	18.1948	0.0004	15.5926	0.0003	38.2844	0.0010	0.856960	0.0005	
	L2	0.05	3.6	–	18.1799	0.0005	15.5613	0.0005	38.2797	0.0010	0.855990	0.0009	
	Augite R	0.433	0.05	15.6589	15.5964	0.0014	14.2103	0.0012	35.7131	0.0030	0.911124	0.0012	
	L1	0.11	5.4	–	18.1944	0.0004	15.5942	0.0004	38.2773	0.0010	0.857100	0.0005	
	L2	0.12	1.9	–	18.1610	0.0006	15.5621	0.0005	38.2511	0.0010	0.856920	0.0006	
	Maskelynite R	0.271	0.88	14.2855	14.2784	0.0004	13.5092	0.0005	34.4298	0.0017	0.946126	0.0011	
	L1	0.05	1.7	–	17.5967	0.0003	15.2247	0.0004	37.6731	0.0010	0.865180	0.0007	
	L2	0.03	6.2	–	16.6188	0.0010	14.6837	0.0010	36.6680	0.0030	0.883560	0.0018	
	Los Angeles	Whole-rock 1 R ^f	0.182	1.4	13.3332	13.3305	0.0030	13.0950	0.0042	33.5057	0.0038	0.982328	0.0038
L1 ^c		0.04	2.5	–	14.2362	0.0025	13.4292	0.0026	34.5356	0.0024	0.943314	0.0010	
L2 ^c		0.02	5.6	–	14.6720	0.0052	13.5818	0.0066	35.0867	0.0063	0.925699	0.0041	
L3 ^c		0.04	0.47	–	13.9273	0.0035	13.3320	0.0039	34.1175	0.0045	0.957254	0.0032	
Whole-rock 2		0.257	0.57	13.5317	13.5182	0.0003	13.1153	0.0004	33.7041	0.0014	0.970194	0.0009	
Whole-rock 3 R		0.28	0.49	–	13.4731	0.0004	13.1280	0.0005	33.5956	0.0016	0.974396	0.0010	
L1+L2		0.18	1.5	–	14.4349	0.0010	13.5064	0.0009	34.6503	0.0024	0.935721	0.0012	
Pigeonite R		0.261	0.22	13.4865	13.4504	0.0003	13.1158	0.0003	33.5127	0.0013	0.975128	0.0009	
L1		0.03	1.4	–	13.8639	0.0009	13.3015	0.0009	34.0012	0.0022	0.959438	0.0012	
L2		0.04	1.1	–	14.0608	0.0006	13.2219	0.0006	34.2388	0.0017	0.940364	0.0009	
Augite R		0.211	0.02	15.1657	14.8538	0.0022	13.9189	0.0020	34.8653	0.0052	0.937062	0.0030	
L1		0.04	1.9	–	13.9178	0.0004	13.2953	0.0004	34.1756	0.0011	0.955351	0.0006	
L2		0.01	1.5	–	13.9175	0.0009	13.2214	0.0009	34.3888	0.0021	0.949986	0.0011	
Maskelynite R		0.342	1.03	13.2491	13.2432	0.0003	13.0492	0.0003	33.3394	0.0011	0.985351	0.0011	
L1		0.05	1.2	–	13.9022	0.0004	13.2570	0.0004	34.1214	0.0014	0.953601	0.0007	
L2		0.03	0.79	–	13.5675	0.0011	13.1083	0.0010	33.7351	0.0030	0.966111	0.0023	
Caliche		0.08	1.12	–	16.3300	0.0006	14.6333	0.0006	36.4829	0.0015	0.895978	0.0013	
Blank composition ENS Lyon, 2007					17.67±0.01		15.55±0.01		37.46±0.01		0.8797±0.0085		

R=residue after leaching.

^a H₂O (L0), 1M HCl (L1), and 3M HF (L2) leachates were analyzed separately for whole-rock, pyroxene, and plagioclase separates. To avoid fractionation of Sm/Nd and Lu/Hf during leaching, the whole-rock powders were analyzed for Pb both unleached and leached when doing Pb work only.

^b Sample weight after leaching for the residues R. See section on analytical techniques for leaching procedures in Bouvier et al. (2005). Leachates were dried and weighed in their respective beakers to estimate Pb concentrations.

^c Pb concentrations estimated from the total Pb ion beam signal during mass spectrometric analysis.

^d Pb isotopic compositions measured by MC-ICP-MS (Nu Plasma HR, Nu Instruments) using a DSN-100 desolvating nebulizer. Pb isotope ratios were corrected for mass bias by the Tl doping and standard bracketing method (Albarède et al., 2004).

^e Blank isotope compositions were measured by mass spectrometry and corrections were applied to some sample Pb isotope ratios. Uncertainties reported on Pb measured isotope ratios are 2σ/√n analytical errors, where n is the number of measured isotopic ratios. Pb–Pb ages were calculated using external reproducibilities on NBS 981 of 400, 500, and 200 ppm (2σ) on ²⁰⁶Pb/²⁰⁴Pb, ²⁰⁷Pb/²⁰⁴Pb, and ²⁰⁷Pb/²⁰⁶Pb, respectively.

^f Los Angeles leached whole-rock fragment #1 from UCLA from Bouvier et al. (2005) reported for comparison with new Pb isotope data on, respectively, unleached and leached whole-rock fragments #2 and #3 from AMNH.

Table 2
Sm–Nd and Lu–Hf mineral and whole-rock isotope data for Shergotty and Los Angeles

Sample	Fraction	Weight (g)	[Sm] ^a (ppm)	[Nd] ^a (ppm)	¹⁴⁷ Sm/ ¹⁴⁴ Nd ^b	¹⁴³ Nd/ ¹⁴⁴ Nd ^b	[Lu] ^c (ppm)	[Hf] ^c (ppm)	¹⁷⁶ Lu/ ¹⁷⁷ Hf ^d	¹⁷⁶ Hf/ ¹⁷⁷ Hf ^d
Shergotty	Whole-rock 1a ^e	–	–	–	–	–	0.183	1.77	0.0146	0.282199±7
	Whole-rock 1b ^e	–	–	–	–	–	0.182	1.77	0.0146	0.282265±25
	Whole-rock 2b	0.140	1.62	4.26	0.2293	0.512333±3	0.261	2.19	0.0169	0.282214±8
	Pigeonite R	0.302	0.209	0.305	0.4148	0.512522±9	0.133	0.977	0.0193	0.282237±7
	Augite R	0.433	0.220	0.332	0.4008	0.512515±6	0.088	0.395	0.0317	0.282280±9
	Maskelynite R	0.271	0.031	0.109	0.1712	0.512244±17	0.007	1.45	0.0006	0.282171±5
Los Angeles	Whole-rock 1 ^f	–	–	–	–	–	0.484	3.02	0.0228	0.282289±3
	Whole-rock 2	0.257	1.69	4.31	0.2368	0.512366±3	0.263	2.05	0.0183	0.282297±4
	Pigeonite R	0.261	0.252	0.362	0.4209	0.512581±5	0.312	3.34	0.0133	0.282280±3
	Augite R	0.211	0.341	0.502	0.4111	0.512567±7	–	–	–	–
	Maskelynite R	0.342	0.029	0.099	0.1804	0.512293±11	0.006	0.905	0.0010	0.282245±3

R=residue after leaching.

^a Nd and Sm isotopic compositions measured by MC-ICP-MS (Nu Plasma HR, Nu Instruments). Errors on Nd and Sm concentrations and on ¹⁴⁷Sm/¹⁴⁴Nd are <0.5% (2σ). Concentrations determined by isotope dilution.

^b Uncertainties reported on Nd measured isotope ratios are 2σ/√n analytical errors in last decimal places, where n is the number of measured isotopic ratios. ¹⁴³Nd/¹⁴⁴Nd normalized for mass fractionation to ¹⁴⁶Nd/¹⁴⁴Nd=0.7219. ¹⁴³Nd/¹⁴⁴Nd of the La Jolla Nd standard=0.511858±18 (2σ) (i.e., external reproducibility=35 ppm). Samples were bracketed with Nd standard analyses. Total procedural blanks for Sm and Nd were <20 pg.

^c Hf and Lu isotopic compositions measured by MC-ICP-MS (Nu Plasma HR, Nu Instruments). Errors on Hf and Lu concentrations and on ¹⁷⁶Lu/¹⁷⁷Hf are <0.5% (2σ). Concentrations determined by isotope dilution.

^d Uncertainties reported on Hf measured isotope ratios are 2σ/√n analytical errors in last decimal place, where n is the number of measured isotopic ratios. ¹⁷⁶Hf/¹⁷⁷Hf normalized for mass fractionation to ¹⁷⁹Hf/¹⁷⁷Hf=0.7325. ¹⁷⁶Hf/¹⁷⁷Hf of the JMC-475 Hf standard=0.282160±0.000010 (2σ) (i.e., external reproducibility=35 ppm). Samples were bracketed with Hf standard analyses. Total procedural blanks for Lu and Hf were <20 pg.

^e Shergotty whole-rock data from Blichert-Toft et al. (1999), fragment #1 from the Smithsonian Institution.

^f Los Angeles whole-rock data from Blichert-Toft et al. (2004). The same fragment #1 of Los Angeles from UCLA was used for the Pb isotope work of Bouvier et al. (2005), data also given in Table 1.

Table 2) is removed from the calculation. The three available measurements on Shergotty whole-rock material (Blichert-Toft et al. (1999) WR1a and WR1b on fragment #1 and this work WR2b on fragment #2 shown in Fig. 1b) justify excluding the whole-rock from the isochron and demonstrate that whole-rock samples from different pieces of the same meteorite do not fall together on a single isochron (Figs. 2a and b). In order to avoid altering the parent/daughter ratios, the whole-rock fragments for these analyses were not leached and, therefore, the compositions that diverge from the isochron most likely reflect contamination or heterogeneous phosphate content from one fragment to another. Lead from the Shergotty unleached whole-rock (WR2b in Table 1) is relatively radiogenic, which may reflect some contamination during handling and curation, in contrast to the leached fragment which lies on the ~4.1 Ga isochron defined previously by Zagami (Fig. 3).

Our Sm–Nd age differs from the previous estimates by Shih et al. (1982) of 620±171 Ma on whole-rock and pyroxene separates and by Jagoutz and Wänke (1986) of 300±50 Ma on leached pyroxene separates, but is consistent with their whole-rock leachate-residue age of

147±20 Ma. The opposite situation was found for the Rb–Sr system (Jagoutz and Wänke, 1986) on maskelynite and pyroxene separates yielding an age of ~167 Ma, while the corresponding whole-rock leachate-residue gave ~360 Ma.

For Los Angeles, the Sm–Nd and Lu–Hf internal isochron ages of, respectively, 181±13 (MSWD=0.14) and 159±42 (MSWD=0.01) are consistent with both the Sm–Nd age of Nyquist and Reese (2000) of 174±12 Ma and the Rb–Sr age of Nyquist et al. (2000) of 165±11 Ma. The Lu–Hf whole-rock composition of Los Angeles as previously measured by Blichert-Toft et al. (2004) on whole-rock fragment #1 (same sample from the University of California Los Angeles (UCLA) collection as used for the Pb isotope work of Bouvier et al., 2005) does not fall on the Lu–Hf internal isochron obtained with the new fragment #2 from AMNH (Figs. 1d and 2).

We present the new Pb isotope data for Shergotty and Los Angeles (Table 1) on the now widely used so-called ‘inverse’ ²⁰⁷Pb/²⁰⁶Pb vs ²⁰⁴Pb/²⁰⁶Pb isochron diagram (Fig. 3) introduced by Tera and Wasserburg (1972) rather than on the ²⁰⁷Pb/²⁰⁴Pb vs ²⁰⁴Pb/²⁰⁶Pb isochron diagram because the effect of the small 204 isotope in the denominator of the latter introduces unwanted noise

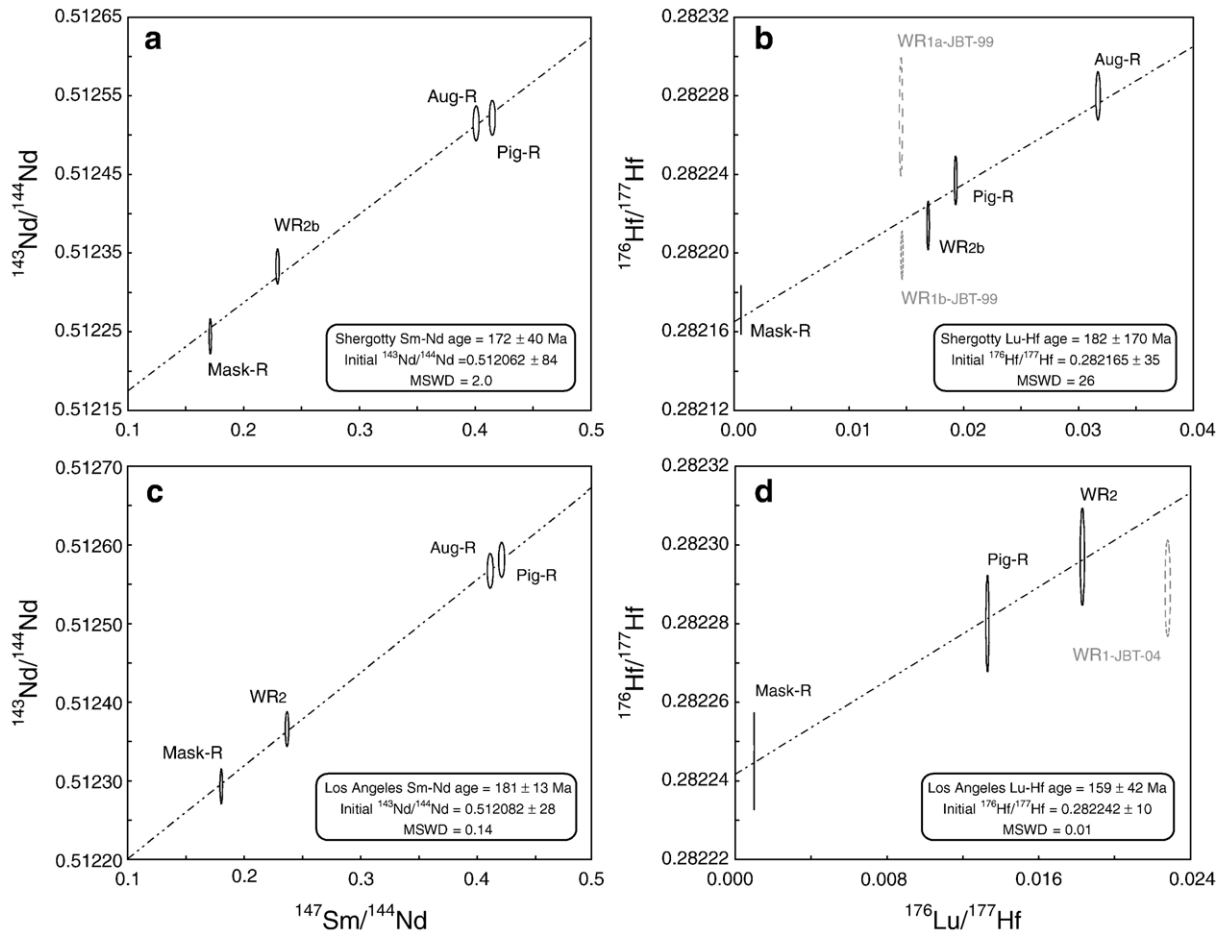


Fig. 1. Sm–Nd and Lu–Hf internal isochrons of Shergotty (a and b) and Los Angeles (c and d). The Lu–Hf whole-rock data for Shergotty and Los Angeles from Blichert-Toft et al. (1999, 2004) are also represented as, respectively, WR1a-JBT-99 and WR1b-JBT-99 for Shergotty and WR1-JBT-04 for Los Angeles (see data in Table 2). The Lu–Hf internal isochron of Shergotty gives 188 ± 24 Ma (MSWD=0.01) if only the three leached mineral separates are regressed.

with non-geological correlation (Debaille et al., 2006). It was demonstrated elsewhere (Albarède et al., 2004) that the correlation coefficient of errors in the $^{207}\text{Pb}/^{206}\text{Pb}$ vs $^{204}\text{Pb}/^{206}\text{Pb}$ correlation diagram is ~ 0.14 and that, in this diagram, the effect of correlated errors therefore is almost negligible.

The Pb isotope compositions of Shergotty and Los Angeles (Table 1) were measured on leached maskelynite and pyroxene (augite and pigeonite) fractions, as well as on leached and unleached whole-rock fragments (annotated, respectively, WR2a and WR2b from the same fragment #2 of Shergotty, and WR1 and WR2 from the fragments #1 and #2 of Los Angeles; see Table 1). For Los Angeles, leached whole-rock material of fragment #1 (WR1) from the UCLA collection was previously analyzed by Bouvier et al. (2005), while the whole-rock fragment #2 from AMNH of this work was

analyzed in its unleached state (due to the simultaneous Sm–Nd and Lu–Hf isotopic work; see section 2) (WR2 in Tables 1 and 2). In addition, small fragments collected during sample cutting at AMNH were leached and dissolved in PFA beakers, and analyzed as an additional leached whole-rock powder (WR3 in Table 1). Fragments of caliche (reddish carbonates formed during the residence of the meteorite in the Mojave desert) were hand-picked from the sample prior to mineral separation and analyzed for their Pb isotope compositions in order to identify potential contaminant compositions. The maskelynite and whole-rock residues from Shergotty and Los Angeles and the pigeonite residue from Los Angeles all fall on the Zagami isochron of Bouvier et al. (2005) (Fig. 3) with $r=0.998$. By contrast, the unleached whole-rock samples of both shergottites, as well as the unleached Shergotty whole-rock sample of

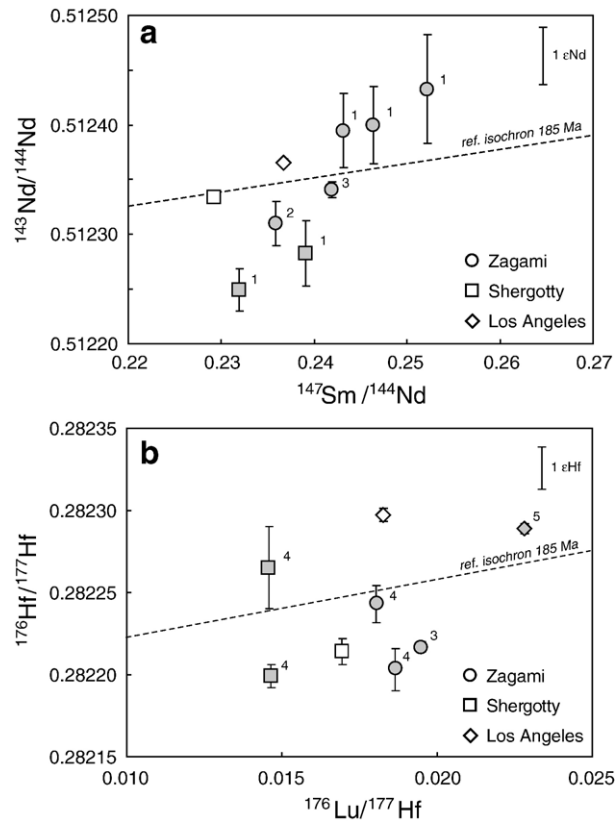


Fig. 2. Sm–Nd (a, upper panel) and Lu–Hf (b, lower panel) isotope compositions of unleached whole-rock fragments of Shergotty, Los Angeles, and Zagami. Isotopic data are from this study (white open symbols) and from the literature (grey filled symbols numbered with the corresponding data source). Sm–Nd and Lu–Hf isochrons corresponding to a 185 Myr slope are shown for reference in both panels. The heterogeneity among the unleached whole-rock fragments of these three shergottites cannot be analytical, but rather reflects the presence of non-cogenetic components. Data from ¹Shih et al. (1982), ²Jagoutz and Wänke (1986), ³Bouvier et al. (2005), ⁴Blichert-Toft et al. (1999), and ⁵Blichert-Toft et al. (2004).

Chen and Wasserburg (1986a,b), and the Los Angeles caliche fall off this isochron, which hints at the presence of a modern contaminant in the interstitial phase. The relatively radiogenic ²⁰⁶Pb/²⁰⁴Pb value of these fractions suggests contamination during either curation, handling, or dissolution in high-pressure PTFE bombs. Likewise, the augite residue of Los Angeles, and the two pyroxene residues from Shergotty also plot off the isochron, a feature already present in the data of Chen and Wasserburg (1986a) on Shergotty, Misawa et al. (1997) on Y-793605, and Borg et al. (2005) on Zagami.

The new data on maskelynite and whole-rock residues from Shergotty and Los Angeles, and the pigeonite residue from Los Angeles define, together with the whole-rock, maskelynite, and pyroxene residues reported by Bouvier et al. (2005) on Zagami, Shergotty, and Los Angeles, an array ('errorchron') with an age of 4055 ± 70 Ma (MSWD=50) (Fig. 3). There was too little Pb present in the Shergotty pigeonite and

augite fractions and in the Los Angeles augite fraction for the results to be significant with respect to contamination (see Borg et al. (2005) Fig. 4 for the Mg-pyroxene and oxide fractions of Zagami). These results are consistent with previous studies on basaltic shergottites by Chen and Wasserburg (1986a) on Shergotty, Zagami, and EETA 79001 and by Borg et al. (2005) on Zagami. Lead in the whole-rock and mineral separate residues of Los Angeles is less radiogenic than in Shergotty and Zagami, which shows that the terrestrial residence of this sample in the desert did not measurably affect the silicate data.

4. Discussion

The new young Sm–Nd and Lu–Hf internal isochron ages for Shergotty and Los Angeles are in accordance with previous findings, including our own. The replicate whole-rock Sm–Nd and Lu–Hf analyses of different

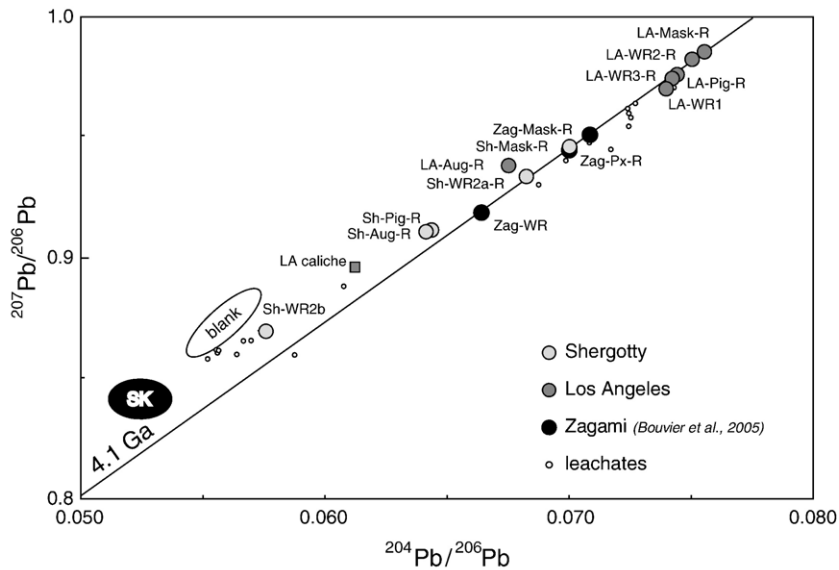


Fig. 3. $^{207}\text{Pb}/^{206}\text{Pb}$ vs $^{204}\text{Pb}/^{206}\text{Pb}$ for unleached and leached whole-rocks and leached mineral separates of Shergotty (Sh) and Los Angeles (LA) (this study), and Zagami (Zag) from Bouvier et al. (2005). All the residues fall on the ~ 4.1 Ga isochron, with the exception of some pyroxene separates from Sh and LA due to their high depletion in Pb compared to the enriched whole-rock and maskelynite separates. WR=whole-rock, Pig=pigeonite, Aug=augite, Mask=maskelynite. SK=modern terrestrial Pb composition from Stacey and Kramers (1975). Field of blank and LA caliche compositions are also represented. Leachate compositions (L0, L1, L2, and L3) of Sh, LA, and Zag are all represented for clarity with the same open symbol.

fragments or powder fractions of a same meteorite, however, do not form alignments with meaningful ages (Figs. 1a–d and 2a and b). The scatter is larger than any

potential inter-laboratory bias and therefore, from the outset, indicates complexities in the Lu–Hf and Sm–Nd isotope systematics, which could include resetting

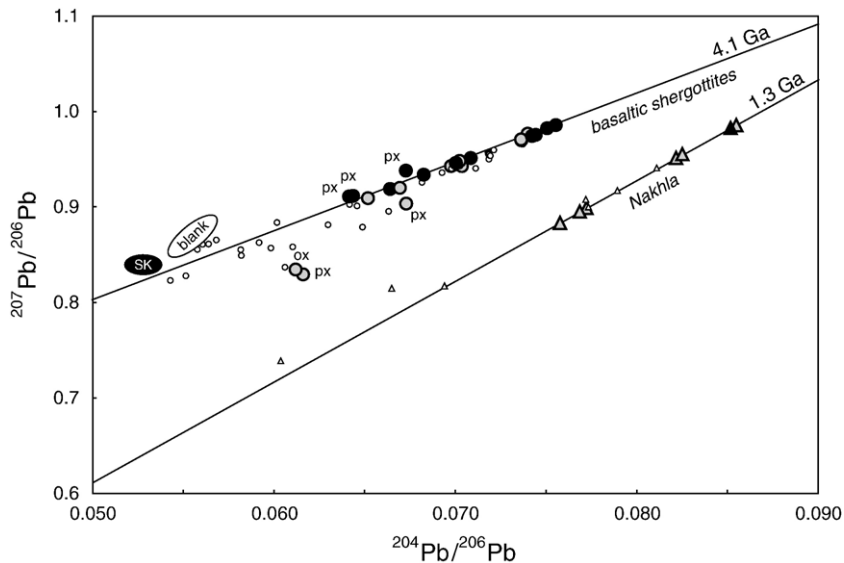


Fig. 4. $^{207}\text{Pb}/^{206}\text{Pb}$ vs $^{204}\text{Pb}/^{206}\text{Pb}$ for leached whole-rocks and mineral separates of the basaltic shergottites Shergotty, Los Angeles, Zagami, and EETA 79001 from this study, Chen and Wasserburg (1986a), Borg et al. (2005), and Bouvier et al. (2005), and of Nakhla from Nakamura et al. (1982), Chen and Wasserburg (1986b), and Bouvier et al. (2005). Data from this study and Bouvier et al. (2005) are represented with black symbols, and data from other studies (Borg et al., 2005; Chen and Wasserburg, 1986a,b; Nakamura et al., 1982) with grey symbols. All the leachates are represented by open symbols. SK=modern terrestrial Pb composition from Stacey and Kramers (1975). Field of blank composition (this work and Bouvier et al. (2005) is also represented.

during shock metamorphism, contamination during handling, initial isotopic heterogeneities, or open system behavior at any time during the history of the sample. Sample heterogeneity likely also plays an important role when the whole-rock fragments analyzed are different pieces from the same meteorite. Sample size, in contrast, does not account for the observed scatter because the combination of unperturbed mineral fractions then should fall on a unique mixing line with a slope still reflecting the age of the last isotopic homogenization (Fig. 2a and b). Whole-rock leachates contain a low- $^{207}\text{Pb}/^{206}\text{Pb}$ component suggestive of either contamination or recent disturbance.

The Pb isotope compositions of leached maskelynite and whole-rocks together with most of the literature data on equivalent samples (Borg et al., 2005; Chen and Wasserburg, 1986a,b) clearly demonstrate that the new Shergotty and Los Angeles data lie on the ~ 4.1 Ga old isochron defined by Zagami (Bouvier et al., 2005) (Fig. 4). The high value of the MSWD (50) is likely the result of a combination of factors: (i) the samples are not all cogenetic, which is consistent with $\delta^{18}\text{O}$ evidence (Clayton and Mayeda, 1983; Franchi et al., 1999); (ii) minor resetting of the U–Pb clock by impacts; and (iii) presence of residual contamination not removed by the mild sample leaching employed during processing.

It first must be noted that none of the internal isochrons from the literature, regardless of the radiometric system used (Rb–Sr, Sm–Nd, Lu–Hf, U–Pb, or Ar–Ar), with the sole exception of Bouvier et al.’s (2005) Pb–Pb results, pass the statistical criteria required to establish the significance of isochrons, unless some phases (leaching and/or residues) are deliberately left out. For example, Jagoutz and Wänke (1986) obtained multiple young internal Rb–Sr and Sm–Nd isochron ages for Shergotty at ~ 170 and 360 Ma, and Borg et al. (1997) and Gaffney et al. (2007) likewise obtained consistently young Rb–Sr, Sm–Nd, and U–Pb ages for QUE 94201 at ~ 330 and 400 Ma. In all of these cases, however, different mineral fractions (residues and/or leachates) were either used or ignored for the various chronometers without strong justification. Regardless, the high level of complexity of the data calls for a correspondingly complex history of the meteorites and thus is a strong indication that the ~ 180 Ma ages date some form of resetting event rather than primary crystallization from isotopically homogeneous melts. A good indicator is that a similar age also is recorded in the shocked chassignite (dunite) NWA 2737: while its Sm–Nd crystallization age is 1.38 ± 0.03 Ga (Misawa et al., 2005), its Ar–Ar age is ~ 160 Ma and is interpreted by the authors to reflect resetting by a “major shock heating event on Mars” (Bogard and Garrison, 2006).

The ancient 4.1 Ga Pb–Pb age as documented in the present work therefore appears fairly robust and we consider that it represents the true emplacement age of these rocks. It further is consistent with the age of 4.1 Ga obtained from the ^{87}Rb – ^{87}Sr errorchron of basaltic, lherzolitic, and olivine-phyric shergottite whole-rock samples (Fig. 5) previously remarked on a smaller set of samples by Shih et al. (1982) and Borg et al. (1997, 2005). Because acid leaching changes the Rb/Sr and potentially also the $^{87}\text{Sr}/^{86}\text{Sr}$ ratios of bulk samples by preferentially removing Sr-rich phosphates, Fig. 5 only shows the data for unleached whole-rocks. We contend that, in agreement with the isotopic similarity between falls and finds (e.g., Zagami and Shergotty vs Los Angeles, NWA 856, and NWA 1195), contamination should not have seriously affected the isochronous relationship of Fig. 5 since shergottites are rich in Sr (14–70 ppm according to Lodders, 1998). Although the 12 shergottites plotted in this figure do not form a

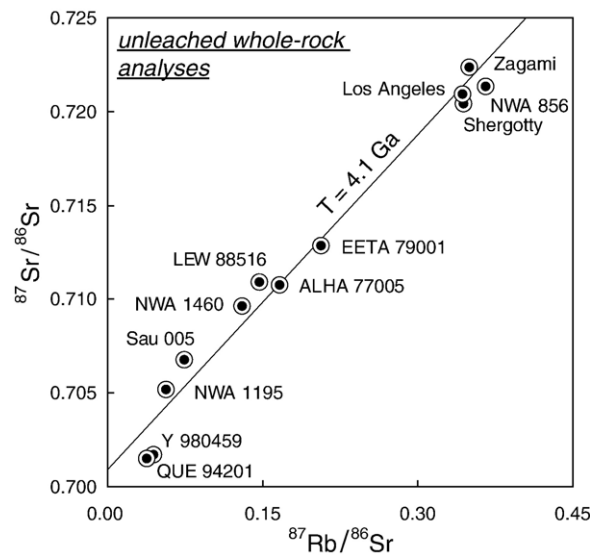


Fig. 5. Whole-rock ^{87}Rb – ^{87}Sr isotopic data on basaltic, lherzolitic, and olivine-phyric shergottites. Only *unleached* samples taken away from fusion crust were considered. The numbers plotted represent the average of existing data (literature or personal communication) for each meteorite. Shergotty (Jagoutz and Wänke, 1986; Nyquist et al., 1979); Zagami (Shih et al., 1982); QUE 94201 (Borg et al., 1997); LEW 88516 (Borg et al., 1998); ALHA 77005 (Shih et al., 1982); Los Angeles (Nyquist et al., 2000); EET79001B (Nyquist et al., 2001; Wooden et al., 1982); NWA 1460 (Nyquist et al., 2004); NWA 856 (Brandon et al., 2004); NWA 1195 (Symes et al., 2005); SaU 005 (Shih et al., 2007); Yamato 980459 (Shih et al., 2004). NWA 1068 (Shih et al., 2003) and SaU 094 (Shih et al., 2007) were not included as they show clear indication of contamination by seawater-like Sr. Whole-rock compositions fall about a ~ 4.1 Ga reference line. The scatter around the reference isochron mostly concerns $^{87}\text{Rb}/^{86}\text{Sr}$ and is an effect of the ~ 170 Ma resetting event.

statistically valid ^{87}Rb – ^{87}Sr isochron, they fall tightly about a 4.1 Ga reference line. The scatter around this line largely results from the small size of the whole-rock samples that were exposed to young isotopic disturbances, which are precisely those events identified by the young internal ^{87}Rb – ^{87}Sr , ^{147}Sm – ^{143}Nd , ^{176}Lu – ^{176}Hf , and U–Pb isochrons.

4.1. Pb contamination and shergottite isotopic components

Gaffney et al. (2007) recently dismissed both Bouvier et al.'s (2005) Pb isotope data on Zagami and other shergottites, and their own 4.3 Ga internal Pb–Pb isochron age obtained on QUE 94201 as reflecting contamination by terrestrial Pb. The core of their argument is that both isochrons intersect the field of terrestrial isotope compositions. Although any Pb–Pb isochron can be considered as a mixing line between radiogenic Pb (on the y-axis) and initial Pb at high $^{204}\text{Pb}/^{206}\text{Pb}$, we will set out in the following to demonstrate that Pb from basaltic shergottites does not form a binary mixture with a component representing a contaminant incorporated on either Earth or Mars. Modern terrestrial Pb (as adequately represented by Stacey and Kramers (1975) in Figs. 3–5) and laboratory blanks plot on or slightly above the Pb–Pb isochron of basaltic shergottites. The samples analyzed by different groups further have been curated by different institutions, but, as pointed out by Bouvier et al. (2005), different groups analyzing the same samples, e.g., Zagami (Borg et al., 2005; Bouvier et al., 2005, Chen and Wasserburg, 1986a, Jagoutz, 1991), have obtained very mutually consistent results. Moreover, most of the samples analyzed so far are falls, but Pb isotope compositions of falls and finds show no systematic differences (e.g., EETA 79001 by Chen and Wasserburg, 1986a). Laboratory contamination therefore should not be an issue as long as the sample/blank ratio is higher than ~ 50 , which is the case of nearly all samples discussed here, in particular the most critical phase, maskelynite. It is further striking that all the shergottite samples plot to the right (i.e., to the unradiogenic side) of common Pb. The Pb isotopic array of shergottites hence cannot be a binary mixture between radiogenic Pb, which should plot on the y-axis, and a component introduced by terrestrial contamination (SK).

Let us therefore examine if instead shergottite Pb could result from a ternary mixture of (i) young radiogenic Pb, (ii) unradiogenic primordial Martian Pb, and (iii) terrestrial contamination (Fig. 6). The challenge here becomes to combine (i.e., homogenize) two of the three components in such a way that the samples remain

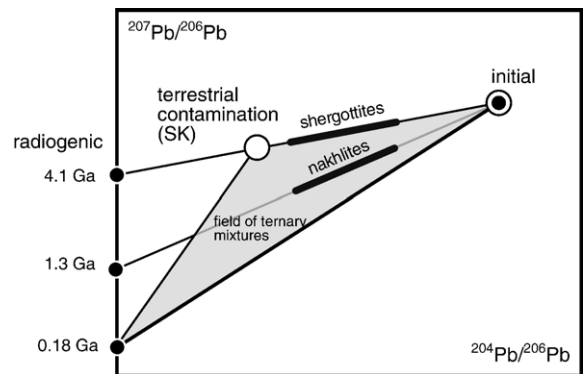


Fig. 6. Schematic illustration of the different potential Pb isotope components: initial, radiogenic, terrestrial, and Martian compared to the Pb isotopic compositions of the shergottite and nakhlite trends. Mixtures of three components, if present in the sample residues, would scatter in the field of ternary mixtures, represented in grey shade. Adding a Pb contaminant to the binary mixture between the initial and the radiogenic components expected for any sample would change the linear array into a scattered set of points, especially for nakhrites which are particularly Pb-poor and form an array which is far removed from modern terrestrial Pb (SK). SK is arbitrarily plotted on top of the shergottite trend as a worse-case scenario.

on a pseudo-binary mixing line rather than scatter over the entire plot. Combining contaminant Pb (iii) with any of the other two types of Pb clearly is unrealistic since in the process both components (i) and (ii) should also have been homogenized. We are therefore left with the last possibility that radiogenic (i) and initial (ii) Pb merged into a unique composition prior to contamination, which is tantamount to assuming that before the shergottites fell on Earth, maskelynite, and presumably other mineral phases as well, were isotopically homogeneous. Such a model is clearly extreme and is falsified by the chemical gradients commonly preserved in a wide range of mineral phases, even for the most labile elements such as Ar (Bogard and Garrison, 1999; Wadhwa et al., 1994). The same analysis applies to contamination by a Martian Pb component, which Borg et al. (2005) claim is visible in leachates and in pyroxene and oxide residues (Fig. 4).

The Pb isotope data for nakhrites provide even stronger evidence against terrestrial contamination. Lead isotopes in Nakhla have been analyzed by a number of groups (Bouvier et al., 2005; Chen and Wasserburg, 1986b; Nakamura et al., 1982). Nakhrites are, on average, much more depleted in Pb than shergottites but, nevertheless, once terrestrial contamination of the Pb-poor phases and potential fusion crust have been taken into account, they define a statistically significant Pb–Pb isochron at ~ 1.3 Ga (Fig. 4), consistent with results from the ^{147}Sm – ^{143}Nd (Nakamura et al., 1982) and ^{39}Ar – ^{40}Ar (Podosek, 1973; Swindle and Olson, 2004) chronometers.

It is difficult to conceive of a contamination process that severely affected shergottites while leaving nakhlites essentially unharmed. For all these reasons, we believe that the two Pb–Pb isochrons on which, respectively, the ~ 4.1 and ~ 1.3 Ga shergottite and nakhlite ages rest do not represent mixing lines with a terrestrial contaminant.

In contrast, if the shergottites were old, a number of striking hyperbolic trends between source μ ($^{238}\text{U}/^{204}\text{Pb}$), P_2O_5 and $\text{mg}\#$ (Blichert-Toft et al., 1999), and La/Yb and $\epsilon_{\text{Nd}}(170 \text{ Ma})$ (Borg et al., 2003) could be explained. It has been argued by Borg et al. (2003) that these hyperbolic arrays, just as the shergottite ^{87}Rb – ^{87}Sr isochron alignment of the whole-rock data about the 4.1 Ga reference line, are mixing artifacts. However, the $^{87}\text{Sr}/^{86}\text{Sr}$ ratios of all of the shergottites recalculated to 4.1 Ga (0.699–0.702) are as would be expected for an old depleted mantle source, whereas special conditions would be required to account for a recent mixing event between young shergottite magmas and undefined lithospheric components. We argue that what was so far considered isotopic component ‘heterogeneity’ merely reflects in situ differential isotopic ingrowth with variable parent/daughter ratios (U/Pb , Lu/Hf , Sm/Nd , Rb/Sr) over a time span of >4 Gyr. We therefore offer the more straightforward alternative interpretation that, taking element compatibilities into account, melting at 4.1 Ga simply would have separated the low-degree melts (e.g., Zagami, Shergotty, Los Angeles,) with high Rb/Sr and U/Pb and low Sm/Nd and Lu/Hf ratios from medium- (e.g., EETA 79001) and high-degree melts (e.g., QUE 94201) of a depleted mantle source with opposite characteristics.

We will now discuss the potential problems associated with interpreting other geochemical observations made on shergottites, notably U–Pb and Ar–Ar data, as supporting young crystallization ages.

4.2. The use of Concordia plots

A number of authors (e.g., Borg et al., 2005; Chen and Wasserburg, 1986b) have plotted U–Pb data for shergottites in Wetherill’s Concordia diagram in which $x = ^{207}\text{Pb}^*/^{235}\text{U}$ and $y = ^{206}\text{Pb}^*/^{238}\text{U}$ with the asterisk designating radiogenic Pb. In order to calculate these values, primordial Pb (approximated by Canyon Diablo Pb) is first subtracted from the measured Pb isotope compositions and the resultant Pb atomic abundances are then divided by the atomic abundances of the relevant U isotopes. This approach was first used by Ulrych (1967) and Allègre (1969) to derive an ‘independent’ age of the Earth from U–Pb data on oceanic basalts. Chen and Wasserburg (1986a) and Borg et al. (2005) also used this approach (or the equivalent Tera–Wasserburg Concor-

dia; Tera and Wasserburg, 1972) to assess their U–Pb data on, respectively, Shergotty and Zagami. The corresponding U–Pb data, however, scatter in an inconsistent way in both the ^{238}U – ^{206}Pb and ^{235}U – ^{207}Pb isochron plots (see Fig. 4 in Borg et al., 2005), indicating that artifacts have compromised the U–Pb systematics in an irrevocable way and thus invalidate the standard interpretation of Concordia alignments. This was pointed out very early on by Oversby et al. (1968). The purpose of the following section is to clarify the issues at stake when using Concordia plots.

First, as pointed out by Amelin et al. (2002), the various techniques of acid leaching used to remove contamination during chemical processing in the laboratory severely disturb absolute U and Pb element abundances. Thus, it is unjustified to assume that measured U/Pb ratios reflect those that prevailed during sample histories and controlled long-term Pb isotopic evolution. Zindler and Jagoutz (1988) noticed that igneous minerals contain mineral and fluid inclusions that can be either avoided or removed by careful mineral separation and leaching. This limitation is particularly critical for shergottites, which contain abundant phosphate, some of which is in the form of minute inclusions in silicate minerals.

Second, the use of the Concordia diagram for viewing relatively unradiogenic samples is fraught with potential artifacts even if the fractionation of U/Pb ratios during leaching could be considered as insignificant. This can be illustrated with the following example, which describes the correspondence between Pb–Pb isochrons and Wetherill’s Concordia plot. Let us make use of the conventional variables of the standard Pb–Pb isochron $\alpha = ^{206}\text{Pb}/^{204}\text{Pb}$ and $\beta = ^{207}\text{Pb}/^{204}\text{Pb}$. The ratio y/x of the Concordia variables $x = ^{207}\text{Pb}^*/^{235}\text{U}$ and $y = ^{206}\text{Pb}^*/^{238}\text{U}$ can be expressed as $1/(^{238}\text{U}/^{235}\text{U})/(^{207}\text{Pb}^*/^{206}\text{Pb}^*) = 1/137.88/(^{207}\text{Pb}^*/^{206}\text{Pb}^*)$ and we can calculate:

$$\frac{^{207}\text{Pb}^*}{^{206}\text{Pb}^*} = \frac{\beta - \beta_{\text{CD}}}{\alpha - \alpha_{\text{CD}}}$$

where the subscript CD refers to Canyon Diablo troilite Pb. The $^{207}\text{Pb}^*/^{206}\text{Pb}^*$ ratio is the *slope* of the line going through the sample and Canyon Diablo. In the so-called ‘inverse’ Pb–Pb isochron diagram β/α vs $1/\alpha$, as used in this work, the equivalent expression is:

$$\frac{^{207}\text{Pb}^*}{^{206}\text{Pb}^*} = \left(\frac{\beta}{\alpha}\right)_{\text{CD}} + \left[\left(\frac{\beta}{\alpha}\right) - \left(\frac{\beta}{\alpha}\right)_{\text{CD}}\right] \frac{(1/\alpha)_{\text{CD}}}{(1/\alpha)_{\text{CD}} - (1/\alpha)}$$

Here, the $^{207}\text{Pb}^*/^{206}\text{Pb}^*$ ratio is the *intercept* of the sample-CD line ($1/\alpha = 0$). The mean $^{207}\text{Pb}^*/^{206}\text{Pb}^*$ value

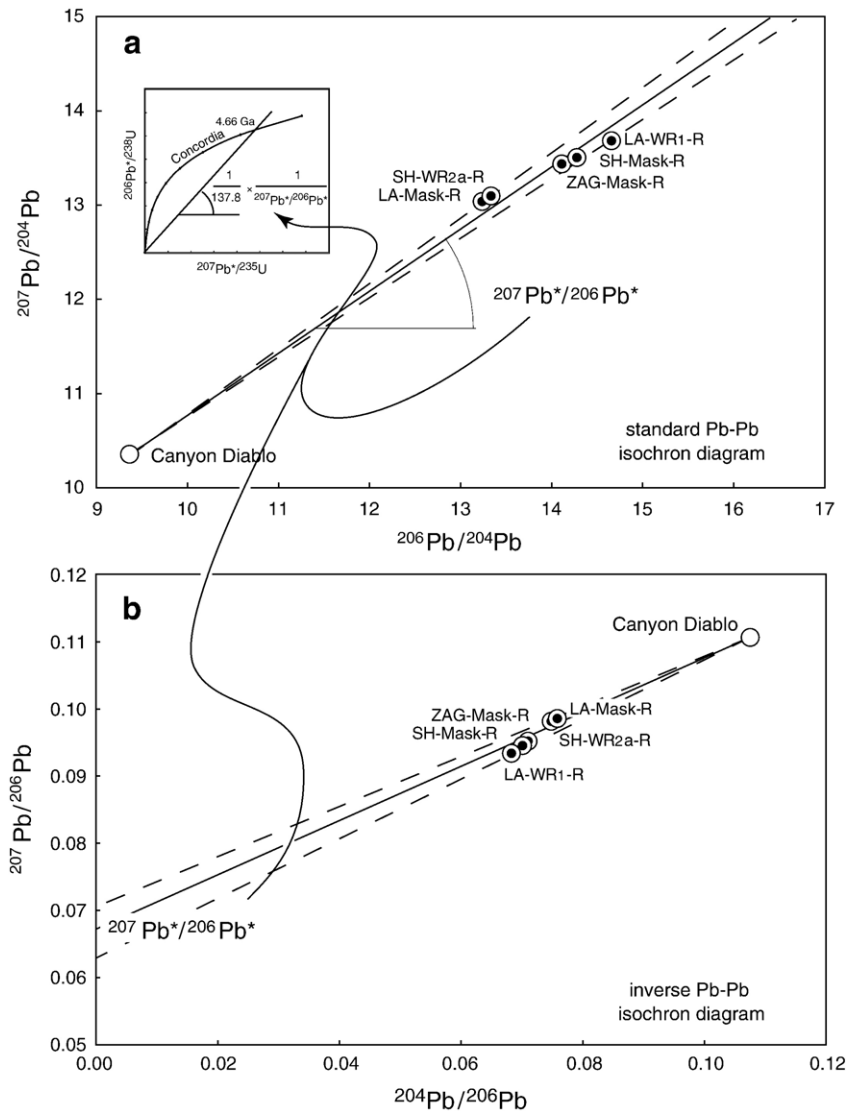


Fig. 7. Correspondence between the standard (top panel a) and inverse (bottom panel b) Pb–Pb isochrons and Wetherill’s Concordia. The main plots show how the Canyon Diablo-corrected $^{207}\text{Pb}^*/^{206}\text{Pb}^*$ of shergottite residues (maskelynite and whole-rocks) (this work and Bouvier et al. (2005)) used in Concordia plots are obtained. The small range of $^{207}\text{Pb}^*/^{206}\text{Pb}^*$ ratios explains why these rocks in a Concordia plot would form a nearly linear array going through zero with an upper intercept equal to the mean $^{207}\text{Pb}^*/^{206}\text{Pb}^*$ age of the group (4.66 Ga) (inset).

of five maskelynite and whole-rock residues of Zagami (Bouvier et al., 2005), Shergotty, and Los Angeles (Table 1 and Fig. 7) is 0.665 with a standard deviation of 0.030 ($\pm 9\%$ deviation at the 95% confidence level). These samples should, therefore, *regardless of their U/Pb ratios*, define in Wetherill’s Concordia plot an alignment that goes through the origin, while the upper intercept with the Concordia will be dominated essentially by the isotopic composition of the initial Pb (CD) and carries no useful chronometric information relevant to the Martian meteorites. In Tera and Wasserburg’s Concordia diagram, the

equivalent alignment should be nearly horizontal (see Chen and Wasserburg’s (1986a) Fig. 5). The apparent age of the ‘upper’ (older) intercept is 4.66 ± 0.13 Ga in agreement with Chen and Wasserburg’s (1986a) results on Zagami. For reference, Chen and Wasserburg (1986a) quoted an upper intercept of 4.59 Ga for Shergotty, while Borg et al.’s (2005) value for Zagami was 4.58 Ga, which again are in agreement with the predicted age. Essentially nothing, therefore, is to be learned from Concordia plots that could not already have been understood from Pb–Pb plots. This line of reasoning justifies why Bouvier et al.

(2005, 2007) chose not to report U and Pb concentrations and why this same option is maintained in the present work.

4.3. The issue of ^{39}Ar – ^{40}Ar ages

Because chronometers based on rare gases are easily reset, evidence of young ages based on the Ar chronometer is particularly relevant to the assessment of old Pb–Pb dates. Bogard and Garrison (1999) reinvestigated the stepwise degassing ^{39}Ar – ^{40}Ar ages of shergottites, while Walton et al. (2007) more recently provided laser-probe data that include various minerals and pockets of shock melts and span a broad range of ages. The challenge of obtaining unambiguous Ar results is made particularly difficult by the presence of cosmogenic Ar, which is most easily observed through the non-planetary proportions of ^{38}Ar and ^{36}Ar . The Ar age spectra of the shergottites are perturbed and yield ages younger than 4.0 Ga: whether these data reflect shocks (Bogard et al., 1979, 1984) or magmatic emplacement (Bogard and Garrison, 1999), however, cannot be resolved from rare gas evidence alone.

A primary problem arising from both the stepwise heating and laser-probe ages is the composition of the non-radiogenic components. Both Bogard and Garrison (1999) and Walton et al. (2007) interpreted their data as indicating the presence of a Martian atmospheric component with a $^{40}\text{Ar}/^{36}\text{Ar}$ ratio of 1700–1900, but which is lower than the ratio (3000 ± 500) measured by the Viking landers (Owen, 1976). Another Ar end-member with $^{40}\text{Ar}/^{36}\text{Ar}$ of ~ 500 was proposed for several shergottites (Bogard and Garrison, 1999; Walton et al., 2007; Wiens, 1988) and interpreted as representing a trapped mantle component. These data are unusual because the $^{40}\text{Ar}/^{36}\text{Ar}$ ratios measured in shergottites are lower than the atmospheric value, a situation which is never encountered for terrestrial samples.

This raises the inescapable question of how a low $^{40}\text{Ar}/^{36}\text{Ar}$ component could have been incorporated into shergottites. On Earth, atmospheric Ar has a $^{40}\text{Ar}/^{36}\text{Ar}$ ratio of 296 and ratios lower than this are not found, especially not in mantle-derived rocks (Allègre et al., 1986), the closest terrestrial equivalents to shergottites. The reason for this is that the isotopic composition of Ar outgassed from the mantle is a function of the timing of that outgassing. Early in the history of the planet, the mantle $^{40}\text{Ar}/^{36}\text{Ar}$ ratio is low when only a small amount of ^{40}Ar has been produced from the decay of ^{40}K and primordial ^{36}Ar dominates. Conversely, the $^{40}\text{Ar}/^{36}\text{Ar}$ ratio is high later in planetary history when abundant ^{40}Ar has been produced. This can be illustrated (Fig. 8)

with a simple box model representing the irreversible degassing of the bulk silicate planet:

$$\frac{d^{36}\text{Ar}}{dt} = -\frac{1}{\tau} {}^{36}\text{Ar} \text{ and}$$

$$\frac{d^{40}\text{Ar}}{dt} = -\frac{1}{\tau} {}^{40}\text{Ar} + \lambda_{\varepsilon} {}^{40}\text{K}_0 e^{-(\lambda_{\beta} + \lambda_{\varepsilon})t}$$

where λ_{β} and λ_{ε} are the decay constants of ^{40}K by beta decay (to ^{40}Ca) and electron capture (to ^{40}Ar), respectively, and τ is the residence time of Ar in the bulk silicate planet (Turner, 1989). If the amount of initial ^{40}Ar present at the time the planet formed with respect to radiogenic ^{40}Ar is neglected and noting $\lambda = \lambda_{\beta} + \lambda_{\varepsilon}$, we obtain:

$$\frac{({}^{40}\text{Ar}/^{36}\text{Ar})_{\text{sil}}}{({}^{40}\text{K}/^{36}\text{Ar})_{\text{sil}}^0} = \frac{\lambda_{\varepsilon} \tau}{\lambda \tau - 1} \frac{e^{-t/\tau} - e^{-\lambda t}}{e^{-t/\tau}}$$

We use the closure condition for each isotope to derive the equation:

$$\frac{({}^{40}\text{Ar}/^{36}\text{Ar})_{\text{atm}}}{({}^{40}\text{K}/^{36}\text{Ar})_{\text{sil}}^0} = \frac{\lambda_{\varepsilon}}{\lambda} \times \left(\frac{\lambda \tau}{\lambda \tau - 1} - \frac{1}{\lambda \tau - 1} \times \frac{1 - e^{-\lambda t}}{1 - e^{-t/\tau}} \right)$$

Fig. 8 shows that, regardless of the residence time τ , the bulk silicate Earth has higher $^{40}\text{Ar}/^{36}\text{Ar}$ ratios than the atmosphere. In the expressions above, we have neglected the initial atmospheric Ar inventory but, since trapped chondritic $^{40}\text{Ar}/^{36}\text{Ar} < 1$ (Huss et al., 1996), its presence would make the atmospheric $^{40}\text{Ar}/^{36}\text{Ar}$ ratio even lower. The very large difference of $^{40}\text{Ar}/^{36}\text{Ar}$ ratios between the Earth's atmosphere and its mantle reveals that the outgassing of Ar into the terrestrial atmosphere occurred rapidly and early in Earth's history (Fig. 8) or perhaps that Ar was present in the atmosphere from the outset. The direction of fractionation is unchanged regardless of the value of τ , even if convection in the Martian mantle is assumed to have been particularly sluggish compared to the Earth. This constraint is extremely difficult to ignore but, remarkably, there is an unchallenged view that somehow it is not valid for Mars.

If Ar in SNCs was controlled by well-defined 'components' (i.e., radiogenic, atmospheric, trapped, and cosmogenic), strong correlations would be identifiable in most Ar isotopic diagrams, which, with some arguable exceptions, is not the case (Bogard and Garrison, 1999; Walton et al., 2007). The reason why we do not see a more well-defined Martian atmospheric component may be due, for example, to the much lower

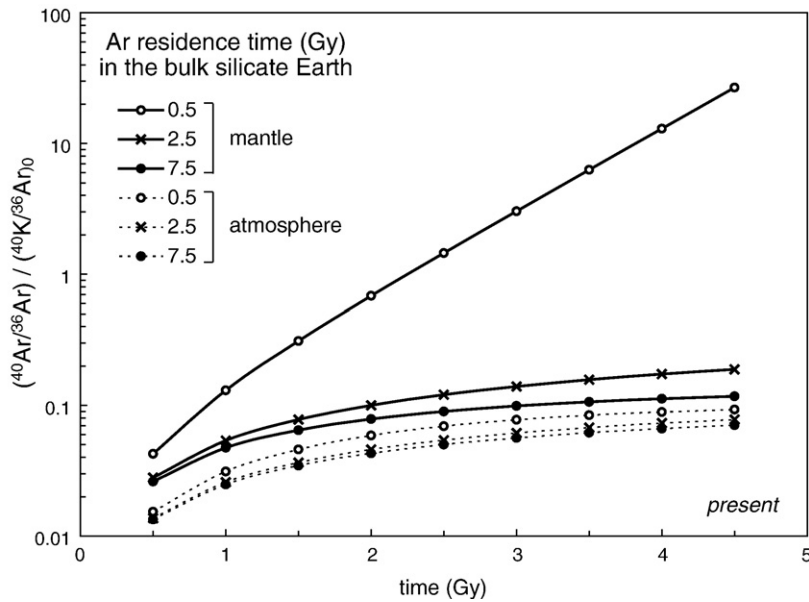


Fig. 8. Argon isotopic evolution of the Earth's mantle (solid lines) and atmosphere (stippled lines) for different Ar residence times of 0.5, 2.5, and 7.5 Gyr in the Bulk Silicate Earth. Slow or fast extraction of Ar from the Earth's mantle does not change the fact that the mantle composition is more radiogenic than the atmosphere. This should also be the case for Mars, which has been active over the first 500 Myr of its history.

pressure of Ar in the Martian atmosphere (a few Pa) (Owen, 1976) compared to that of the Earth (~ 1000 Pa). Much of the Ar may actually have been acquired by the Martian atmosphere through meteorite impacts (Owen, 1992), but too little is known about meteorite fluxes to quantify this. A crude but realistic strategy therefore is to neglect the atmospheric contribution to sample ^{40}Ar , and to assume that most, if not all, ^{36}Ar in samples is of cosmogenic origin. The $^{40}\text{Ar}/^{39}\text{Ar}$ ratios, especially those associated with high $^{40}\text{Ar}/^{36}\text{Ar}$ ratios, can then be directly translated into apparent ages. The assumption of negligible unradiogenic (Martian atmosphere or trapped) ^{40}Ar indeed provides ^{39}Ar – ^{40}Ar ages surprisingly consistent with those obtained by other techniques for both Nakhla and Lafayette (1328 ± 15 Ma and 1322 ± 10 Ma respectively; Nakamura et al., 1982; Podosek, 1973; Swindle and Olson, 2004), Chassigny (1.32 ± 0.07 Ga; Bogard and Garrison, 1999; Jagoutz, 1996), and, to a lesser extent, ALH 84001 (~ 4.3 Ga; Bogard and Garrison, 1999; Nyquist et al., 1995), but all these meteorites have experienced lower shock pressures (5 to 30 GPa) than shergottites (20 to 55 GPa) (Fritz et al., 2005). The same assumption also results in rather old ^{39}Ar – ^{40}Ar ages for feldspars from the shergottites QUE 94201 (600–800 Ma) and EETA 79001 (2.4–3.4 Ga) and for most ^{39}Ar – ^{40}Ar SNC ages obtained on matrix minerals by laser probe by Walton et al. (2007). We note that both Bogard and Garrison (1999) and Walton et al. (2007) decline to interpret these old shergottite dates as

being meaningful and instead assign them to an effect of trapped Ar, but do not provide independent evidence to support this interpretation.

The laser-probe Ar–Ar ages (uncorrected for atmospheric contamination) obtained for melt pockets in shergottites are also old (Walton et al., 2007). Melt pockets are objects that form when shock energy is focused on tiny domains. Fig. 9 shows that 23 of the ^{39}Ar – ^{40}Ar ages of melt pockets in Los Angeles, Zagami, NWA 1068, and DaG 476 are very old (~ 700 – 4500 Ma), though not unacceptably old, i.e. >4.5 Ga. There is essentially no correlation between the ^{39}Ar – ^{40}Ar ages calculated without atmospheric correction and the $^{40}\text{Ar}/^{36}\text{Ar}$ ratios, which would be expected if a non-radiogenic ^{40}Ar component, such as implanted atmospheric Ar, was present. This is particularly apparent for the data from Los Angeles. For Zagami and NWA 1068, the melt pockets with the highest $^{40}\text{Ar}/^{36}\text{Ar}$ ratios (Zagami #22 and #26; NWA 1068 #22 and #32) also have extremely high $^{39}\text{Ar}/^{36}\text{Ar}$ ratios, implying that enough ^{40}K is present to support most or all of the ^{40}Ar signal. The broad range of $^{40}\text{Ar}/^{36}\text{Ar}$ ratios observed for the melt pockets (430–3300) encompasses the atmospheric value (3000 ± 500) measured by the Viking landers (Owen, 1992), but its lower part requires an additional source of ^{36}Ar . Bogard and Garrison (1999) and Walton et al. (2007) suggest that this source is a trapped mantle component with $^{40}\text{Ar}/^{36}\text{Ar} \sim 500$. For the reasons explained above, however, it is unlikely that

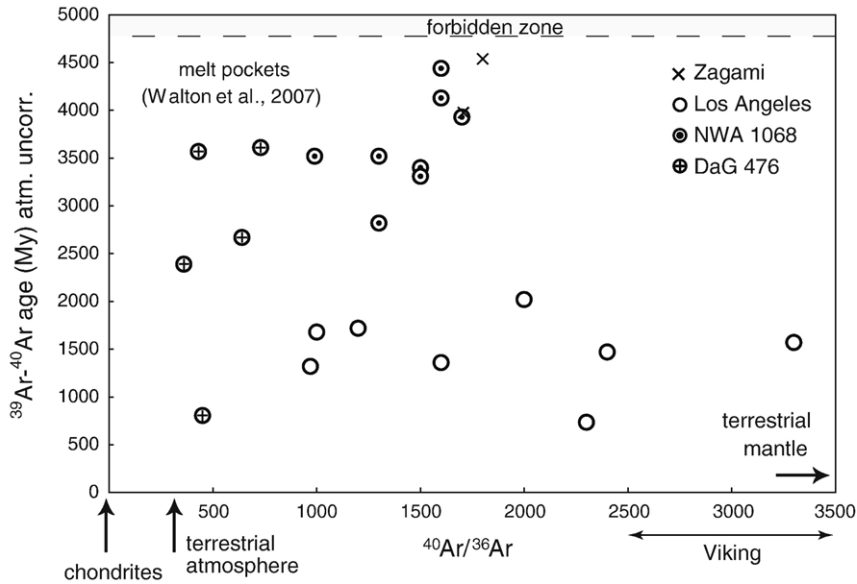


Fig. 9. ^{39}Ar – ^{40}Ar ages uncorrected for the atmospheric component vs $^{40}\text{Ar}/^{36}\text{Ar}$ ratios of melt pockets in Los Angeles, Zagami, NWA 1068, and DaG 476 from Walton et al. (2007). Argon with Martian atmospheric composition ($^{40}\text{Ar}/^{36}\text{Ar}=3000\pm 500$ measured by the Viking lander) trapped during impact events is not correlated with old ages. Martian atmospheric Ar also gives a strict inferior limit for the Martian mantle composition as nothing is found on Earth with a lower $^{40}\text{Ar}/^{36}\text{Ar}$ than the terrestrial atmospheric composition (~ 296).

trapped mantle Ar would be *less* radiogenic than atmospheric Ar, and a recent estimate of ~ 2000 for the Martian interior Ar by Schwenzer et al. (2007) further discredits the previous value. We prefer the alternative explanation which holds that a nearly pure ^{36}Ar -rich component with $^{40}\text{Ar}/^{36}\text{Ar}\ll 1$ was implanted by chondritic impactors (Huss et al., 1996), in addition to traces of atmospheric gases. Such a mechanism preserves the ^{39}Ar – ^{40}Ar ages calculated without atmospheric correction just as for the nakhlites and Chassigny. Both stepwise and laser-probe ^{39}Ar – ^{40}Ar results therefore affirm that ages much older than 180 Ma are definitely discernible in shergottites.

4.4. Can U–Pb ages on baddeleyite solve the conundrum?

It has recently been suggested that baddeleyite (ZrO_2), an accessory but ubiquitous mineral in plutonic rocks such as gabbros, may help unravel the chronological conundrum of shergottites (Herd et al., 2007; Misawa and Yamaguchi, 2007). Baddeleyite occasionally is used for U–Pb dating when zircon is absent. An excellent example was provided by the U–Pb data acquired by Söderlund et al. (2004) on mafic dykes with the purpose of calibrating the controversial ^{176}Lu decay constant with respect to U–Pb ages (and thus the well-defined ^{235}U and ^{238}U decay constants). Let us first point out that the largest dimension of baddeleyite crystals in shergottites is about

10 μm , meaning that the diameter of both the laser beam used by Herd et al. (2007) and the ion beam used by Misawa and Yamaguchi (2007) largely encroaches on neighboring minerals. The significance of baddeleyite U–Pb and Pb–Pb ages therefore is very ambiguous. In addition, the *status* of this mineral in shergottites also is particularly unclear. It is generally accepted that baddeleyite crystallizes from the late-stage interstitial liquids of basaltic magmas. This fact together with their high U concentrations and lack of common Pb at the time of crystallization, as well as the apparently low diffusivity of Pb with respect to this mineral, makes baddeleyite an excellent substitute for zircons when these have not reached their saturation level in a given magma, such as is commonly the case for basaltic liquids. Herd et al. (2007) reported very imprecise, but definitely very young ages for ~ 10 micron-sized baddeleyite crystals present in Zagami, NWA 3171, NWA 1460, and DaG 476 (e.g., 70 ± 35 Ma for Zagami and 171 ± 129 Ma for NWA 3171).

Baddeleyite, however, also is well known as a mineral that forms in impact melts. El Goresy (1965) and Marvin and Kring (1992) reported a variety of occurrences of this mineral, which apparently results from the decomposition of zircon (ZrSiO_4) into ZrO_2 and silica glass (SiO_2). This subject was recently reviewed by Wittmann et al. (2006), who also provided microphotographs to document the process in question. It is notable that the type of shock environment envisioned here precisely defines the habitus

of baddeleyite in the shergottites described by Herd et al. (2007), in which ZrO_2 , silica glass, melt pockets, and maskelynite coexist. Kerschhofer et al. (2000) investigated the phase changes between ZrO_2 polymorphs taking place at up to 25 GPa and 2500°C. Temperature and pressure conditions during shock metamorphism are rather well known due to the presence of high-pressure phases, such as stishovite, hollandite, and perovskite (Beck et al., 2005; Langenhorst and Poirier, 2000a,b). The most common estimates of 25 GPa for Shergotty were recently increased by Sharp et al. (1999), who observed the presence of a post-stishovite phase formed above 45 GPa. Moreover, a maximum shock pressure of 55 GPa was assigned to ALHA 77005 by Fritz et al. (2005). Under these conditions, baddeleyite crystals as observed in shergottites are not primary minerals and cannot be depicted as simple late-stage magmatic minerals. If they grew as baddeleyite in the first place, they must since have gone through several successive phase changes, presumably monoclinic and orthorhombic I (or tetragonal) forms at >3 GPa, followed by the orthorhombic II form at >15 GPa (Kerschhofer et al., 2000). Some of the shergottite-hosted baddeleyites, in particular those associated with high-silica glass, also could have resulted from zircon decomposition (Wittmann et al., 2006). In either case, we consider such conditions inappropriate to the preservation of a closed system for the U–Pb chronometer in <10 micron-wide crystals. The diffusion parameters that would allow an accurate closure temperature to be calculated are missing, but crystals as small as those described by Herd et al. (2007) (3–10 μm) should equilibrate with their surroundings at relatively low temperatures. Baddeleyite, rather than dating magmatic crystallization, actually may help constrain the age of shock events happening at the surface of Mars.

4.5. Old shergottites from an old Martian surface

The assertion of old (~4.1 Ga) magmatic ages for basaltic shergottites raises important questions about the significance of the younger radiogenic isotope ages (e.g., the ~180 Ma ages and more infrequently those at ~475 Ma; Nyquist et al., 2001). If the young ages date shock metamorphism, they must correspond to an event of widespread importance on the planet and one that could be explained by mechanisms operating in the inner Solar System. One such possibility recently has been suggested by Bottke et al. (2007). Using various dynamical models, they found compelling evidence that a 170 km diameter carbonaceous chondrite-like asteroid *Baptistina*, which belonged to the Flora asteroid family formed at ~450–500 Ma (Nesvorný et al., 2005),

broke up 150 ± 20 Myr ago in the innermost region of the main asteroid belt. Approximately 15–20% of this body's multi-kilometer fragments were directly injected (or drifted by Yarkovsky thermal forces) into resonance with Jupiter, where they would have been thrown into Mars-crossing (and Earth-crossing) orbits (Nesvorný et al., 2002). These events correspond well to the young age clusters measured in shocked shergottites.

Alternatively, the young events recorded by shergottites may correspond to the last dry-out of large Martian lakes (Bouvier et al., 2005). The 'drying-lake' model is supported by the ~1‰ range of $\delta^{18}\text{O}$ values observed for SNC whole-rock samples (Clayton and Mayeda, 1983; Franchi et al., 1999), which cannot result from magmatic processes. It is also consistent with hydrogen isotope data (Leshin et al., 1996) and more specifically with recent work on apatites from shergottites. These show very high D/H values ($\delta D = 3500\text{--}4600\text{‰}$; Greenwood et al., 2007) characteristic of modern Martian atmospheric hydrogen ($\delta D = 4000\text{‰}$) as measured by the Viking landers (Owen, 1992), but clearly heavier than Martian magmatic water ($\delta D = 900\text{‰}$; Leshin, 2000) and water from clinopyroxene and feldspathic glass of shergottites ($\delta D = -50$ to $+1300\text{‰}$; Boctor and Alexander, 2007). The D/H data are entirely consistent with a scenario of resetting by percolating fluids, possibly slightly acidic (i.e., sulfuric acid), of the chronometers hosted by apatite (i.e., Rb–Sr, Sm–Nd, Lu–Hf, U–Pb), which occurs in shergottites as either isolated crystals or inclusions in the major mineral phases (Bouvier et al., 2005).

A very old shergottite age has strong implications for the interpretation of extinct radioactivities and convection in the Martian mantle. Shergottites have a large range of $\epsilon^{142}\text{Nd}$ ($T_{1/2} = 103$ Myr) values varying from -0.2 to $+0.9$ (variation in parts per 10,000), but only little variability in $\epsilon^{182}\text{W}$ ($T_{1/2} = 9$ Myr) is observed (around $0.4 \epsilon^{182}\text{W}$; Foley et al., 2005; Kleine et al., 2004). This indicates that the shergottite mantle source was still heterogeneous at the time of melting, which in turn may indicate that either convection did not have enough time to stir the Martian mantle sufficiently to erase the original heterogeneities or the shergottite parent magmas originated from within an ancient lithosphere. To some extent, the ^{142}Nd isotopic signature of shergottites mirrors the 3.8 Ga old metabasalts from Isua, West Greenland, which show $\epsilon^{142}\text{Nd}$ values of $\sim +0.15$ with respect to the Bulk Silicate Earth (BSE), whereas modern terrestrial rocks show no variability in ^{142}Nd abundances (Boyet et al., 2003; Boyet and Carlson, 2005; Caro et al., 2003, 2006). In terms of extinct radioactivities, the 1.3 Ga old nakhlites and chassignites can be taken as

relatively recent samples of Bulk Silicate Mars (BSM) and serve as a reference for the other samples. They have non-chondritic ^{142}Nd and ^{182}W abundances indicative of a strong depletion of their source in incompatible elements with respect to the Earth while ^{146}Sm and ^{182}Hf were still extant ($\epsilon^{142}\text{Nd} \sim +0.8$ and $\epsilon^{182}\text{W} \sim +2.5$; Foley et al., 2005; Kleine et al., 2004). Since chondrites have values of $\epsilon^{142}\text{Nd} \sim -0.2$ and $\epsilon^{182}\text{W} \sim -2$ (Boyet and Carlson, 2005; Kleine et al., 2002; Yin et al., 2002), BSM seems to be more depleted than BSE. This strong depletion of the Martian mantle in incompatible elements is apparent also in the modern Nd and Hf isotope compositions of nakhlites and lherzolic and basaltic shergottites (Blichert-Toft et al., 1999, 2004). As proposed for the Earth (Blichert-Toft and Albarède, 1997; Boyet and Carlson, 2005; Chase and Patchett, 1988), such depletion may be explained by either a non-chondritic planet or very early formation of crust subsequently recycled and buried in the deep mantle or lithosphere, either of which then remained isolated from the convection system for at least the first three billion years of the planet's history (forming the so-called hidden reservoir). Loss of an enriched primordial crust to space during or shortly after accretion is another possible interpretation (Albarède, 1998). A major difference between Mars and the Earth is that for Mars samples with negative $\epsilon^{142}\text{Nd}$ values are known, which is not the case for the Earth: these are the basaltic shergottites Zagami and Shergotty, which may represent parent magmas produced by remelting of this early reservoir 4.1 Gyr ago.

Hartmann and Barlow (2006) discuss why young shergottite ages could be consistent with the crater size-frequency chronology of the planet (Barlow, 1988; Hartmann and Neukum, 2001) and favor an effect of the lithology on meteorite launch efficiency. Werner (2005), however, identified 18 large impact basins with ages between 3.7 and 4.1 Ga (most of them in the interval 4.0–4.1 Ga), which confirm earlier inferences (e.g., Barlow, 1988; Hartmann and Neukum, 2001) that most of the heavily cratered terrains of the Southern Hemisphere were present during Noachian times (pre-3.7 Ga). Hartmann and Barlow (2006) assess that $\sim 40\%$ of the Martian surface is of Noachian age but this figure is misleading because it leaves out terrains affected by fluvial, eolian, and impact resurfacing, all processes that are unrelated to magmatic crystallization ages. The issue of secondary cratering is relevant mostly to the dating of younger surfaces. Overall, a very consistent picture now emerges when crater chronology and shergottite Pb–Pb ages are put together. Moreover, the ~ 4.1 Ga age of shergottites also is consistent with their extinct radioactivity anomalies and with an active dyna-

mo and mantle convection on Mars during the first 500 Myr of its history. It is remarkable that no true basalt has yet been recognized among the SNCs: even if some shergottites are labeled 'basaltic' they are still crystalline, occasionally coarse-grained, and none of them even remotely resembles an aa or pahoehoe lava of the type that is observed at, for example, Hawaiian volcanoes. Given that true fast-cooled basalts exist among lunar meteorites (e.g., Fagan et al., 2002), this should be taken as an indication that only the most energetic impacts can dig out SNCs and that these rocks therefore come from well below the surface.

5. Conclusions

Our new Pb isotope data on Shergotty and Los Angeles combined with our previous Pb data on Zagami and Pb data from the literature define an isochron indicating that shergottites crystallized ~ 4.1 Gyr ago. The conflict between different isotopic systems is only apparent from and boils down to a contrast between mineral and whole-rock isochron ages. The old Pb–Pb age is in agreement with evidence drawn from the whole-rock ^{87}Rb – ^{87}Sr systematics of shergottites. In contrast, the young ages obtained from Rb–Sr, Sm–Nd, Lu–Hf, and U–Pb internal isochrons reflect a later perturbation, due either to shock metamorphism during impact or resetting of phosphate during the aqueous alteration of these rocks. Ar–Ar ages of SNCs and U–Pb ages of shocked baddeleyite crystals date impacts that recently affected different sites on the Martian surface. The new 4.1 Ga age of shergottites is consistent with crater counting chronology and also reconciles evidence of extant short-lived radioactivities and an active dynamo and mantle convection on Mars at the time the shergottites formed.

Acknowledgements

We are grateful to the curating committee of the Muséum National d'Histoire Naturelle in Paris and to Denton Ebel at the American Museum of Natural History in New York for donating samples of, respectively, Shergotty and Los Angeles. We thank Alan Brandon, Larry Nyquist, Chi-Yu Shih, and Steven Symes for generously providing some of their unpublished Rb–Sr data in tabulated form. We further are indebted to Philippe Telouk for assistance with the Nu Plasma and to Chantal Douchet for day-to-day maintenance of the clean lab at ENSL. AB is thankful to Yulia Goreva and Dante Lauretta for making available the clean lab facilities at the Lunar and Planetary Laboratory in Tucson and to Jon Patchett for allowing her

to dedicate some of her time to this work. Discussions with Pierre Beck, William Bottke, and Ahmed El Goresy were much appreciated. This work was carried out with financial support from the French National Programme for Planetology (PNP). Comments by Bill Hartmann and Thorsten Kleine were particularly useful.

Appendix A. Supplementary data

Supplementary data associated with this article can be found, in the online version, at doi:10.1016/j.epsl.2007.1.006.

References

- Albarède, F., 1998. Mantle convection and geochemical hideouts. EOS Trans AGU Fall Meeting 79, A#S12E-01.
- Albarède, F., Télouk, P., Blichert-Toft, J., Boyet, M., Agranier, A., Nelson, B., 2004. Precise and accurate isotopic measurements using multiple-collector ICP-MS. *Geochim. Cosmochim. Acta* 68, 2725–2744.
- Allègre, C.J., 1969. Comportement des systèmes U–Th–Pb dans le manteau supérieur et modèle d'évolution de ce dernier au cours des temps géologiques. *Earth Planet. Sci. Lett.* 5, 261–269.
- Allègre, C.J., Staudacher, T., Sarda, P., 1986. Rare gas systematics: formation of the atmosphere, evolution and structure of the Earth's mantle. *Earth Planet. Sci. Lett.* 81, 127–150.
- Amelin, Y., Krot, A.N., Hutcheon, I.D., Ulyanov, A.A., 2002. Lead isotopic ages of chondrules and calcium–aluminum-rich inclusions. *Science* 297, 1679–1683.
- Barlow, N.G., 1988. Crater size-frequency distributions and a revised Martian relative chronology. *Icarus* 75, 285–305.
- Beck, P., Gillet, P., El Goresy, A., Mostefaoui, S., 2005. Timescales of shock processes in chondritic and martian meteorites. *Nature* 435, 1071–1074.
- Blichert-Toft, J., Albarède, F., 1997. The Lu–Hf isotope geochemistry of chondrites and the evolution of the mantle–crust system. *Earth Planet. Sci. Lett.* 148, 243–258.
- Blichert-Toft, J., Boyet, M., Albarède, F., 2004. Further Lu–Hf and Sm–Nd isotopic data on planetary materials and consequences for planetary differentiation. *Lunar Planet. Sci. Conf. XXXV*, A1226.
- Blichert-Toft, J., Gleason, J.D., Télouk, P., Albarède, F., 1999. The Lu–Hf isotope geochemistry of shergottites and the evolution of the Martian mantle–crust system. *Earth Planet. Sci. Lett.* 173, 25–39.
- Boctor, N.Z., Alexander, C.M.O'D., 2007. Volatile Abundances and H Isotope Signature of Feldspathic Glass and Clinopyroxene in the Shergottites Zagami, EETA 79001, Shergotty, and ALHA 77005. *Lunar Planet. Sci. Conf. XXXVIII*, A1801.
- Bogard, D.D., Johnson, C.L., 1983. Martian gases in an Antarctic meteorite? *Science* 221, 651–654.
- Bogard, D.D., Nyquist, L.E., Johnson, P., 1984. Noble gas contents of shergottites and implications for the Martian origin of SNC meteorites. *Geochim. Cosmochim. Acta* 48, 1723–1739.
- Bogard, D.D., Garrison, D.H., 1999. Argon–39–argon–40 “ages” and trapped argon in Martian shergottites, Chassigny, and Allan Hills 84001. *Meteorit. Planet. Sci.* 34, 451–473.
- Bogard, D.D., Garrison, D.H., 2006. Ar–Ar Dating of Martian Chassignites, NWA2737 and Chassigny, and Nakhilite MIL03346. *Lunar Planet. Sci. Conf. XXXVII*, A1108.
- Bogard, D.D., Husain, L., Nyquist, L.E., 1979. 40Ar–39Ar age of the Shergotty achondrite and implications for its post-shock thermal history. *Geochim. Cosmochim. Acta* 43, 1047–1055.
- Borg, L.E., Edmunson, J.E., Asmerom, Y., 2005. Constraints on the U–Pb isotopic systematics of Mars inferred from a combined U–Pb, Rb–Sr, and Sm–Nd isotopic study of the Martian meteorite Zagami. *Geochim. Cosmochim. Acta* 69, 5819–5830.
- Borg, L.E., Nyquist, L.E., Taylor, L.A., Wiesmann, H., Shih, C.-Y., 1997. Constraints on Martian differentiation processes from Rb–Sr and Sm–Nd isotopic analyses of the basaltic shergottite QUE 94201. *Geochim. Cosmochim. Acta* 61, 4915–4931.
- Borg, L.E., Nyquist, L.E., Wiesmann, H., 1998. Rb–Sr isotopic systematics of ilherzolitic shergottite LEW88516. *Lunar Planet. Sci. Conf. XXIX*, A1233.
- Borg, L.E., Nyquist, L.E., Wiesmann, H., Shih, C., Reese, Y., 2003. The age of Dar al Gani 476 and the differentiation history of the martian meteorites inferred from their radiogenic isotope systematics. *Geochimica and Cosmochimica Acta* 67, 3519–3536.
- Bottke, W.F., Vokrouhlicky, D., Nesvorný, D., 2007. An asteroid breakup 160 Myr ago as the probable source of the K/T impactor. *Nature* 449, 48–53.
- Bouvier, A., Blichert-Toft, J., Vervoort, J.D., Albarède, F., 2005. The age of SNC meteorites and the antiquity of the Martian surface. *Earth Planet. Sci. Lett.* 240, 221–233.
- Bouvier, A., Blichert-Toft, J., Moynier, F., Vervoort, J.D., Albarède, F., 2007. Pb–Pb dating constraints on the accretion and cooling history of chondrites. *Geochim. Cosmochim. Acta* 71, 1583–1604.
- Boyet, M., Blichert-Toft, J., Rosing, M., Storey, M., Télouk, P., Albarède, F., 2003. ¹⁴²Nd evidence for early Earth differentiation. *Earth Planet. Sci. Lett.* 214, 427–442.
- Boyet, M., Carlson, R.W., 2005. ¹⁴²Nd Evidence for Early (>4.53 Ga) Global Differentiation of the Silicate Earth. *Science* 309, 576–581.
- Brandon, A.D., Nyquist, L.E., Shih, C., Wiesmann, H., 2004. Rb–Sr and Sm–Nd Isotope Systematics of Shergottite NWA 856: Crystallization Age and Implications for Alteration of Hot Desert SNC Meteorites. *Lunar Planet. Sci. Conf. XXXV*, A1931.
- Caro, G., Bourdon, B., Birck, J.-L., Moorbath, S., 2003. ¹⁴⁶Sm–¹⁴²Nd evidence from Isua metamorphosed sediments for early differentiation of the Earth's mantle. *Nature* 423, 428–432.
- Caro, G., Bourdon, B., Birck, J.L., Moorbath, S., 2006. High-precision ¹⁴²Nd/¹⁴⁴Nd measurements in terrestrial rocks: constraints on the early differentiation of the Earth's mantle. *Geochim. Cosmochim. Acta* 70, 164–191.
- Chase, C.G., Patchett, P.J., 1988. Stored mafic/ultramafic crust and early Archean mantle depletion. *Earth Planet. Sci. Lett.* 91, 66–72.
- Chen, J.H., Wasserburg, G.J., 1986a. Formation ages and evolution of Shergotty and its parent planet from U–Th–Pb systematics. *Geochim. Cosmochim. Acta* 50, 955–968.
- Chen, J.H., Wasserburg, G.J., 1986b. S (not Equal To) N (maybe Equal) C. *Lunar Planet. Sci. Conf. XVII*, A113–A114.
- Clayton, R.N., Mayeda, T.K., 1983. Oxygen isotopes in eucrites, shergottites, nakhlites, and chassignites. *Earth Planet. Sci. Lett.* 62, 1–6.
- Connerney, J.E.P., Acuña, M.H., Wasilewski, P.J., Kletetschka, G., Ness, N.F., Rème, H., Lin, R.P., Mitchell, D.L., 2001. The Global Magnetic Field of Mars and Implications for Crustal Evolution. *Geophys. Res. Lett.* 28, 4015–4018.
- Debaille, V., Blichert-Toft, J., Agranier, A., Doucelance, R., Schiano, P., Albarède, F., 2006. Geochemical component relationships in MORB from the Mid-Atlantic Ridge, 22–35°N. *Earth Planet. Sci. Lett.* 241, 844–862.
- El Goresy, A., 1965. Baddeleyite and its significance in impact glasses. *J. Geophys. Res.* 70, 3454–3465.

- Fagan, T.J., Taylor, G.J., Keil, K., Bunch, T.E., Wittke, J.H., Korotev, R.L., Jolliff, B.L., Gillis, J.J., Haskin, L.A., Jarosewich, E., Clayton, R.N., Mayeda, T.K., Fernandes, V.A., Burgess, R., Turner, G., Eugster, O., Lorenzetti, S., 2002. Northwest Africa 032: Product of lunar volcanism. *Meteorit. Planet. Sci.* 37, 371–394.
- Foley, C.N., Wadhwa, M., Borg, L.E., Janney, P.E., Hines, R., Grove, T.L., 2005. The early differentiation history of Mars from ^{182}W – ^{142}Nd isotope systematics in the SNC meteorites. *Geochim. Cosmochim. Acta* 69, 4557–4571.
- Franchi, I.A., Wright, I.P., Sexton, A.S., Pillinger, C.T., 1999. The oxygen-isotopic composition of Earth and Mars. *Meteorit. Planet. Sci.* 34, 657–661.
- Fritz, J., Artemieva, N., Greshake, A., 2005. Ejection of Martian meteorites. *Meteorit. Planet. Sci.* 40, 1393–1411.
- Gaffney, A.M., Borg, L.E., Connelly, J., 2007. Uranium-lead isotope systematics of Mars inferred from the basaltic shergottite QUE 94201. *Geochim. Cosmochim. Acta* 71, 5016–5031.
- Greenwood, J.P., Itoh, S., Sakamoto, N., Vicenzi, E.P., Yurimoto, H., 2007. Hydrogen isotopography of apatite in Los Angeles, Shergotty, and ALH 84001: new constraints on Martian water history and SNC petrogenesis. *Lunar Planet. Sci. Conf. XXXVIII*, A1338.
- Harper Jr., C.L., Nyquist, L.E., Bansal, B., Wiesmann, H., Shih, C.-Y., 1995. Rapid accretion and early differentiation of Mars indicated by $^{142}\text{Nd}/^{144}\text{Nd}$ in SNC meteorites. *Science* 267, 213–217.
- Hartmann, W.K., Barlow, N.G., 2006. Nature of the Martian uplands: effect on Martian meteorite age distribution and secondary cratering. *Meteorit. Planet. Sci.* 41, 1453–1467.
- Hartmann, W.K., Neukum, G., 2001. Cratering chronology and the evolution of Mars. *Space Sci. Rev.* 96, 165–194.
- Herd, C.D.K., Simonetti, A., Peterson, N.D., 2007. In Situ U–Pb Geochronology of Martian Baddeleyite by Laser Ablation MC-ICP-MS. *Lunar Planet. Sci. Conf. XXXVIII*, A1664.
- Huss, G.R., Lewis, R.S., Hemkin, S., 1996. The “normal planetary” noble gas component in primitive chondrites: compositions, carrier, and metamorphic history. *Geochim. Cosmochim. Acta* 60, 3311–3340.
- Jagoutz, E., 1991. Chronology of SNC meteorites. *Space Sci. Rev.* 56, 13–22.
- Jagoutz, E., 1996. Nd isotopic systematics of Chassigny. *Lunar Planet. Sci. Conf. XXVII*, A597.
- Jagoutz, E., Wänke, H., 1986. Sr and Nd isotopic systematics of Shergotty meteorite. *Geochim. Cosmochim. Acta* 50, 939–953.
- Jones, J.H., 1986. A discussion of isotopic systematics and mineral zoning in the shergottites: evidence for a 180 m.y. igneous crystallization age. *Geochim. Cosmochim. Acta* 50, 969–977.
- Kerschhofer, L., Schärer, U., Deutsch, A., 2000. Evidence for crystals from the lower mantle: baddeleyite megacrysts of the Mbuji Mayi kimberlite. *Earth Planet. Sci. Lett.* 179, 219–225.
- Kleine, T., Mezger, K., Münker, C., Palme, H., Bischoff, A., 2004. ^{182}Hf – ^{182}W isotope systematics of chondrites, eucrites, and martian meteorites: chronology of core formation and early mantle differentiation in Vesta and Mars. *Geochim. Cosmochim. Acta* 68, 2935–2946.
- Kleine, T., Münker, C., Mezger, K., Palme, H., 2002. Rapid accretion and early core formation on asteroids and the terrestrial planets from Hf–W chronometry. *Nature* 418, 952–955.
- Langenhorst, F., Poirier, J.-P., 2000a. ‘Eclogitic’ minerals in a shocked basaltic meteorite. *Earth Planet. Sci. Lett.* 176, 259–265.
- Langenhorst, F., Poirier, J.-P., 2000b. Anatomy of black veins in Zagami: clues to the formation of high-pressure phases. *Earth Planet. Sci. Lett.* 184, 37–55.
- Lee, D.-C., Halliday, A.N., 1997. Core formation on Mars and differentiated asteroids. *Nature* 388, 854–857.
- Leshin, L.A., Epstein, S., Stolper, E.M., 1996. Hydrogen isotope geochemistry of SNC meteorites. *Geochim. Cosmochim. Acta* 60, 2635–2650.
- Leshin, L.A., 2000. Insights into martian water reservoirs from analyses of martian meteorite QUE94201. *Geophys. Res. Lett.* 27, 2017–2020.
- Lodders, K., 1998. A survey of shergottite, nakhlite and chassigny meteorites whole-rock compositions. *Meteorit. Planet. Sci.* 33, 183–190.
- Ludwig, K.R., 2001. Isoplot/Ex version 2.49. A Geochronological Toolkit for Microsoft Excel., Berkeley Geochronology Center Special Publ. 1a. November 20.
- Marvin, U.B., Kring, D.A., 1992. Authentication controversies and impactite petrography of the New Quebec Crater. *Meteoritics* 27, 585–595.
- Mathew, K.J., Marty, B., Marti, K., Zimmermann, L., 2003. Volatiles (nitrogen, noble gases) in recently discovered SNC meteorites, extinct radioactivities and evolution. *Earth. Planet. Sci. Lett.* 214, 27–42.
- Misawa, K., Nakamura, N., Premo, W.R., Tatsumoto, M., 1997. U–Th–Pb isotopic systematics of lherzolitic shergottite Yamato-793605. *Antarct. Meteorite Res.* 10, 95–108.
- Misawa, K., Shih, C.-Y., Reese, Y., Nyquist, L.E., Barrat, J.-A., 2005. Rb–Sr and Sm–Nd Isotopic Systematics of NWA 2737 Chassignite. *Meteorit. Planet. Sci.* 40, A5200.
- Misawa, K., Yamaguchi, A., 2007. U–Pb Ages of NWA 856 Baddeleyite. *Meteorit. Planet. Sci.* 42, A5228.
- Nakamura, N., Unruh, D.M., Tatsumoto, M., 1982. Origin and evolution of the Nakhla meteorite inferred from the Sm–Nd and U–Pb systematics and REE, Ba, Sr, Rb and K abundances. *Geochim. Cosmochim. Acta* 46, 1555–1573.
- Nesvorný, D., Morbidelli, A., Vokrouhlický, D., Bottke, W.F., Broz, M., 2002. The Flora family: a case of the dynamically dispersed collisional swarm? *Icarus* 157, 155–172.
- Nesvorný, D., Vokrouhlický, D., Bottke, W.F., 2005. the breakup of a main-belt asteroid 450 thousand years ago. *Science* 312, 1490.
- Nyquist, L.E., Bansal, B., Wiesmann, H., Shih, C.-Y., 1995. Martians young and old: Zagami and ALH 84001. *Lunar Planet. Sci. Conf. XXVI*, A1065–A1066.
- Nyquist, L.E., Bogard, D.D., Shih, C., Greshake, A., Stöfler, D., Eugster, O., 2001. Ages and geologic histories of Martian meteorites. *Space Sci. Rev.* 96, 105–164.
- Nyquist, L.E., Borg, L.E., Shih, C.-Y., 1998. The Shergottite age paradox and the relative probabilities for Martian meteorites of differing ages. *J. Geophys. Res.* 103, 31445–31455.
- Nyquist, L.E., Reese, Y.D., 2000. Dating Desert Meteorites: The Los Angeles Experience. AGU Fall Meeting, A #P51A-02.
- Nyquist, L.E., Reese, Y.D., Wiesmann, H., Shih, C.-Y., Schwandt, C., 2000. Rubidium–strontium age of the Los Angeles Shergottite. *Meteorit. Planet. Sci.* 35.
- Nyquist, L.E., Shih, C., Reese, Y., Irving, A.J., 2004. Crystallization age of NWA 1460 Shergottite: paradox revisited. Second conference on early Mars: geologic, hydrologic, and climatic evolution and the implications for life, A8041.
- Nyquist, L.E., Wooden, J., Bansal, B., Wiesmann, H., McKay, G., Bogard, D.D., 1979. Rb–Sr age of the Shergotty achondrite and implications for metamorphic resetting of isochron ages. *Geochim. Cosmochim. Acta* 43, 1057–1074.
- Oversby, V.M., Gast, P.W., Ulrych, T.J., 1968. Oceanic basalt leads and the age of the Earth. *Science* 162, 925–928.
- Owen, T., 1976. Volatile inventories on Mars. *Icarus* 28, 171–177.
- Owen, T., 1992. The composition and early history of the atmosphere of Mars, in Mars (A93-27852 09-91), pp. 818–834.

- Pepin, R.O., 1985. Evidence of Martian origins. *Nature* 317, 473–475.
- Podosek, F.A., 1973. Thermal history of the nakhlites by the ^{40}Ar – ^{39}Ar method Earth Planet. Sci. Lett. 19, 135–144.
- Rajan, R.S., Lugmair, G.W., Tamhane, A.S., Poupeau, G., 1986. Nuclear tracks, Sm isotope and neutron capture effects in Elephant Moraine shergottite. *Geochim. Cosmochim. Acta* 50, 1039–1042.
- Schwenzer, S.P., Herrmann, S., Mohapatra, R.K., Ott, U., 2007. Noble gases in mineral separates from three Shergottites: Shergotty, Zagami, and EETA79001. *Meteorit. Planet. Sci.* 42, 387–412.
- Sharp, T.G., El Goresy, A., Wopenka, B., Chen, M., 1999. A post-stishovite SiO_2 polymorph in the meteorite Shergotty: implications for impact events. *Science* 284, 1511–1513.
- Shih, C.-Y., Nyquist, L.E., Bogard, D.D., McKay, G.A., Wooden, J.L., Bansal, B.M., Wiesmann, H., 1982. Chronology and petrogenesis of young achondrites, Shergotty, Zagami, and ALHA77005: late magmatism on a geologically active planet. *Geochim. Cosmochim. Acta* 46, 2323–2344.
- Shih, C., Nyquist, L.E., Reese, Y., 2007. Rb–Sr and Sm–Nd isotopic studies of Martian depleted shergottites SaU 094/005. *Lunar Planet. Sci. Conf. XXXVIII*, A1745.
- Shih, C., Nyquist, L.E., Wiesmann, H., Barrat, J.A., 2003. Age and petrogenesis of picritic shergottite NWA 1068: Sm–Nd and Rb–Sr isotopic studies. *Lunar Planet. Sci. Conf. XXXIV*, A1439.
- Shih, C., Nyquist, L.E., Wiesmann, H., Misawa, K., 2004. Rb–Sr and Sm–Nd Isotopic Studies of Shergottite Y980459 and a petrogenetic link between depleted Shergottites and Nakhlites. *Lunar Planet. Sci. Conf. XXXV*, A1814.
- Söderlund, U., Patchett, P.J., Vervoort, J.D., Isachsen, C.E., 2004. The ^{176}Lu decay constant determined by Lu–Hf and U–Pb isotope systematics of Precambrian mafic intrusions. *Earth Planet. Sc. Lett.* 219, 311–324.
- Stacey, J.S., Kramers, J.D., 1975. Approximation of terrestrial lead isotope evolution by a two-stage model. *Earth Planet. Sci. Lett.* 26, 207–221.
- Swindle, T.D., Olson, E.K., 2004. ^{40}Ar – ^{39}Ar studies of whole rock nakhlites: evidence for the timing of formation and aqueous alteration on Mars. *Meteorit. Planet. Sci.* 39, 755–766.
- Symes, S.J., Borg, L.E., Shearer, C.K., Asmerom, Y., Irving, A.J., 2005. Geochronology of NWA 1195 based on Rb–Sr and Sm–Nd isotopic systematics. *Lunar Planet. Sci. Conf. XXXVI*, A1435.
- Tanaka, K.L., Scott, D.H., 1987. Eruptive history of the Elysium volcanic province of Mars. NASA, Washington, Reports of Planetary Geology and Geophysics Program, 1986, pp. 333–335.
- Tanaka, K.L., Scott, D.H., Greeley, R., 1992. Global stratigraphy 345–382.
- Tera, F., Wasserburg, G.J., 1972. U–Th–Pb systematics in lunar highland samples from the Luna 20 and Apollo 16 missions. *Earth Planet. Sci. Lett.* 17, 36–51.
- Turner, G., 1989. The outgassing history of the Earth's atmosphere. *J. Geol. Soc. London.* 146, 147–154.
- Ulrych, T.J., 1967. Oceanic basalt leads: a new interpretation and an independent age for the Earth. *Science* 158, 252–256.
- Wadhwa, M., McSween Jr., H.Y., Crozaz, G., 1994. Petrogenesis of shergottite meteorites inferred from minor and trace element microdistributions. *Geochim. Cosmochim. Acta* 58, 4213–4229.
- Walton, E.L., Kelley, S.P., Spray, J.G., 2007. Shock implantation of Martian atmospheric argon in four basaltic shergottites: A laser probe Ar/Ar investigation. *Geochim. Cosmochim. Acta* 71, 497–520.
- Weiss, B.P., Vali, H., Baudenbacher, F.J., Kirschvink, J.L., Stewart, S.T., Shuster, D.L., 2002. Records of an ancient Martian magnetic field in ALH84001. *Earth Planet. Sci. Lett.* 201, 449–463.
- Werner, S.C., 2005. Major Aspects of the Chronostratigraphy and Geologic Evolutionary History of Mars. PhD dissertation, Freie Universität Berlin.
- Werner, S.C., Ivanov, B.A., Neukum, G., 2005. The Martian crater size-frequency distribution and the evolutionary history of Mars. *Amer. Astro. Soc.* 691, 691.
- Wiens, R.C., 1988. Noble gases released by vacuum crushing of EETA 79001 glass. *Earth Planet. Sci. Lett.* 91, 55–65.
- Wittmann, A., Kenkmann, T., Schmitt, R.T., Stöffler, D., 2006. Shock-metamorphosed zircon in terrestrial impact craters. *Meteorit. Planet. Sci.* 41, 433–454.
- Wooden, J.L., Shih, C.-Y., Nyquist, L.E., Bansal, B.M., Wiesmann, H., McKay, G., 1982. Rb–Sr and Sm–Nd isotopic constraints on the origin of EETA 79001: a second Antarctic shergottite. *Lunar Planet. Sci. Conf. XIII*, A879–A880.
- Yin, Q., Jacobsen, S.B., Yamashita, K., Blichert-Toft, J., Télouk, P., Albarède, F., 2002. A short timescale for terrestrial planet formation from Hf–W chronometry of meteorites. *Nature.* 418, 949–952.
- Zindler, A.G., Jagoutz, E., 1988. Mantle cryptology. *Geochim. Cosmochim. Acta* 52, 319–333.